LAWRENCE
LIVERMORE
NATIONAL
LABORATORY

LLNL-JRNL-610212

Super-grid modeling of the elastic wave equation in semi-bounded domains

N. A. Petersson, B. Sjogreen

January 15, 2013

Communications in Computational Physics

Disclaimer

Super-grid modeling of the elastic wave equation in semi-bounded domains

N. Anders Petersson* and Björn Sjögreen*

January 11, 2013

Abstract

We develop a super-grid modeling technique for solving the elastic wave equation in semi-bounded two- and three-dimensional spatial domains. In this method, a coordinate mapping is used to transform a very large physical domain to a significantly smaller computational domain, where the elastic wave equation is solved numerically on a regular grid. To damp out waves that become poorly resolved because of the coordinate mapping, a high order artificial dissipation operator is added in layers near the boundaries of the computational domain. We prove by energy estimates that the super-grid modeling leads to a stable numerical method with decreasing energy, which is valid for heterogeneous material properties and a free surface boundary condition on one side of the domain. Our spatial discretization is based on a fourth order accurate finite difference method, which satisfies the principle of summation by parts. We show that the summation by parts property holds when a centered finite difference stencil is combined with homogeneous Dirichlet conditions at several ghost points outside of the far-field boundaries. Therefore, the coefficients in the finite difference stencils need only be boundary modified near the free surface. This allows for improved computational efficiency and significant simplifications of the implementation of the proposed method in multi-dimensional domains. Numerical experiments in three space dimensions show that the modeling error from truncating the domain can be made very small by choosing a sufficiently wide super-grid damping layer. The numerical accuracy is evaluated against analytical solutions of Lamb's problem, where we demonstrate that a sixth order artificial dissipation results in a fourth order accurate solution for long time simulations. We also observe very small artificial reflections for the layer over halfspace (LOH1) test problem, where a heterogeneous material model is used.

1 Introduction

To numerically solve a time-dependent wave equation in an unbounded spatial domain, it is necessary to truncate the domain and impose a far-field closure at, or near, the boundaries of the truncated domain. Numerous different approaches have been suggested, see for example [4, 7, 15]. The perfectly matched layer (PML) technique, originally proposed by Berenger [3] and later improved by many others, has been very successful for electromagnetic wave simulations. Unfortunately, the PML technique has stability problems

*Center for Applied Scientific Computing, L-422, LLNL, P.O. Box 808, Livermore, CA 94551, USA.
This work performed under the auspices of the U.S. Department of Energy by Lawrence Livermore National Laboratory under Contract DE-AC52-07NA27344. This is contribution LLNL-JRNL-XXXYYY.

for the elastic wave equation, where free surface boundaries and material discontinuities can form wave guides in which the solution of the PML system becomes unstable [17]. The PML system is also known to exhibit stability problems for some anisotropic wave equations [2].

In this article, we use the super-grid approach [1] combined with fourth order accurate summation by parts operators [16] to derive a stable and accurate numerical method for wave equations on unbounded domains. Similar to the PML technique, the super-grid method modifies the original wave equation in layers near the boundary of the computational domain. The PML system is defined by Fourier transforming the original wave equation in time and applying a frequency-dependent complex-valued coordinate transformation in the layers. Additional dependent variables, governed by additional differential equations, must be introduced to define the PML system in the time domain. In comparison, the super-grid method is based on applying a real-valued coordinate stretching in the layers, where also artificial dissipation is added. The super-grid method does not rely on additional dependent variables, and is therefore more straight forward to implement. The super-grid method is energy stable if there is an energy estimate for the underlying wave equation. In particular, we prove that the super-grid method is stable for the elastic wave equation with heterogeneous material properties and free surface boundary conditions. The super-grid approach does not guarantee perfect absorption of all traveling waves. However, we will demonstrate by numerical experiments that the errors due to artificial reflections can be made to be as small as the propagation errors due to truncation errors in the interior scheme.

The stability theory is first presented for the scalar wave equation in one spatial dimension. It is then generalized to the half-plane problem for the two-dimensional elastic wave equation in a heterogeneous isotropic material. The reflection properties of the super-grid method are evaluated by solving Lamb's problem, where the numerical solution can be compared to an analytical solution. Here a point force acts on the free surface of a three-dimensional homogeneous half-space. The half-space problem subject to a free surface condition permits surface waves, which are of significant importance in applications such as seismology and seismic exploration. Surface waves only propagate along the free surface and decay exponentially away from the surface, and are fundamentally different from the longitudinal and transverse waves that travel through the volume of the domain. Surface waves therefore constitute a third type of wave that need to be absorbed by the far-field closure.

We are primarily interested in cases where the solution is of a transient nature, being driven by initial data with compact support, or a forcing function that only is active (non-zero) for a limited time. Assume that we wish to calculate the numerical solution in the bounded subdomain $\bar{\Omega} \in \mathrm{R}^d$, where $d = 1, 2$, or 3. For $d = 3$ this could, for example, be a box shaped domain $\bar{\Omega} = \{x_1 \le x \le x_2,\ y_1 \le y \le y_2,\ z_1 \le z \le z_2\}$, where (x, y, z) are the Cartesian coordinates. Also assume that we wish to calculate the numerical solution in the finite time interval $0 \le t \le t_{max}$. A straight forward (but naive) approach would be to make the computational domain larger in all directions and perform the numerical calculation on an extended domain $x_1 - L \le x \le x_2 + L$, etc. Due to the hyperbolic nature of wave equations, reflections from the outer boundary can only pollute the solution in the subdomain $\bar{\Omega}$ for times $t > t_L = 2L/c_{max}$, where c_{max} is the largest phase velocity in the domain. Hence, by choosing $L \ge t_{max}\, c_{max}/2$, we can avoid all artifacts from the truncation of the extended domain, up to time $t = t_{max}$. Unfortunately, this simple

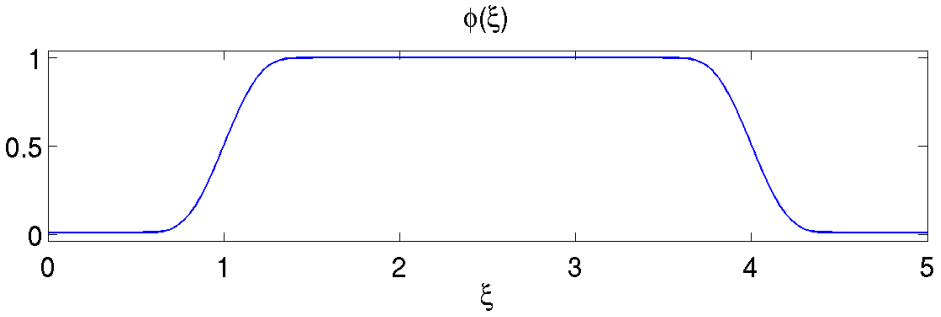

Figure 1: *The taper function $\phi^{(x)}(\xi)$ is used to compress the extended domain to a much smaller computational domain. Here, the domain of interest is $1.5 \leq \xi \leq 3.5$ and the width of each layer is $\ell = 1.5$.*

approach is computationally intractable, because the size of the extended domain grows with t_{max} and could easily become much larger than the original domain of interest.

The first ingredient of the super-grid approach [1] is to introduce a smooth coordinate transformation,

$$x = X(\xi), \quad y = Y(\eta), \quad z = Z(\zeta),$$

that maps the computational domain onto a much larger extended domain. For example, in the x-direction, $x_1 - \ell \leq \xi \leq x_2 + \ell$ is mapped onto $x_1 - L \leq x \leq x_2 + L$, where $\ell \ll L$. The original wave equation is solved inside the domain of interest, i.e., the identity mapping $x = \xi$ is used for $x_1 \leq \xi \leq x_2$. The parts of the computational domain that are *outside* of the domain of interest are called the super-grid layers, i.e., $x_1 - \ell \leq \xi < x_1$ and $x_2 < \xi \leq x_2 + \ell$.

Spatial derivatives in the wave equation are transformed according to the chain rule,

$$\frac{\partial}{\partial x} = \phi^{(x)}(\xi)\frac{\partial}{\partial \xi}, \quad \frac{\partial}{\partial y} = \phi^{(y)}(\eta)\frac{\partial}{\partial \eta}, \quad \frac{\partial}{\partial z} = \phi^{(z)}(\zeta)\frac{\partial}{\partial \zeta}, \tag{1}$$

where

$$\phi^{(x)}(\xi) = \frac{1}{X'(\xi)}, \quad \phi^{(y)}(\eta) = \frac{1}{Y'(\eta)}, \quad \phi^{(z)}(\zeta) = \frac{1}{Z'(\zeta)}.$$

To make the coordinate transformation non-singular, we assume $\phi^{(q)} \geq \varepsilon_L > 0$, $q = x, y, z$.

For a one-dimensional Cauchy problem, $\phi^{(x)}$ needs to be a smooth function that transitions monotonically from ε_L to 1 between $x_1 - \ell$ and x_1, and then back to ε_L between x_2 and $x_2 + \ell$, see Figure 1. For higher dimensional problems, the functions $\phi^{(y)}$ and $\phi^{(z)}$ are defined in a corresponding way.

In the mapped (computational) coordinates, the length scale of the solution in the ξ-direction is proportional to $\phi^{(x)}$. The solution is therefore compressed inside the layers, where $\phi^{(x)} < 1$. This corresponds to a slowing down of all traveling waves in the mapped coordinates. Note that in a two-dimensional domain, $\phi^{(x)} < 1$ corresponds to a slow down in the ξ-direction, while $\phi^{(y)} < 1$ gives a slow down in the η-direction. Hence, if the original wave equation has isotropic wave propagation properties, it will become

anisotropic in the mapped coordinates. The case of a half-plane problem in two space dimensions is illustrated in Figure 2.

Figure 2: *A two-dimensional half-plane domain with a physical boundary along the top edge. The stretching functions satisfy* $\phi^{(x)} = \phi^{(y)} = 1$ *in the white region, where the original wave equation is solved. The wave speed is reduced in the surrounding layers by taking* $\phi^{(x)} < 1$ *(red) and* $\phi^{(y)} < 1$ *(blue). In the purple corner regions,* $\phi^{(x)} < 1$ *and* $\phi^{(y)} < 1$.

The super-grid method discretizes the mapped (computational) domain on a grid with constant size. For this reason, the resolution in terms of grid points per wave length will be very poor in the layers. To avoid polluting the numerical solution by modes that can not be resolved on the grid, the second essential ingredient of the super-grid method is the addition of artificial damping. Note that the dissipative term is only added in the layers. The idea is to damp out poorly resolved waves before they arrive at the outer edge of the layer, where the computational domain is truncated. As was emphasized in [1], it is important to use a damping term of sufficiently high order, such that its strength does not dominate the truncation error in the interior of the domain, or reduce the stability limit of the explicit time step.

For half-plane problems, only one side of the computational domain has a physical boundary. All other sides of the computational domain are part of the far-field boundary closure. Note that we have freedom in choosing what boundary conditions to impose along these boundaries, as long as they do not cause any instabilities.

Stability of our explicit time-stepping scheme for the elastic wave equation hinges on the summation by parts (SBP) property of the spatial discretization [16]. Ghost points, located outside the boundary, are used to enforce the boundary conditions strongly. We therefore call our discretization technique SBP-GP to emphasize the differences with SBP-SAT [10, 9], which uses penalty terms to enforce the boundary conditions weakly. The SBP-GP technique prescribes how the centered difference operators must be modified near the boundary and gives a matching discretization of the boundary conditions. For a fourth order SBP-GP method with heterogeneous material properties, the coefficients in the difference formulas are modified in the first six grid points next to the boundary [16]. In principle, we could use the boundary modified operators in all directions of the domain, but such an approach leads to complicated difference stencils in several space dimensions, with many special cases near sides, edges, and corners of the computational domain. A much simpler and more computationally efficient discretization is obtained if we instead

use centered difference stencils all the way up to the far-field boundaries. A centered fourth order accurate discretization of the wave equation uses a five point stencil, which needs boundary conditions at two consecutive ghost points. Two ghost points are also sufficient if a fourth order dissipation operator is used in the super grid layers, but more ghost points are needed for higher order artificial dissipation. In this paper we show that the SBP property holds without boundary modifications, when Dirichlet boundary conditions are imposed at those ghostpoints, guaranteeing stability of the proposed approach.

The remainder of the paper is organized in the follwing way. In Section 2, we analyze the one-dimensional scalar wave equation with super-grid layers and derive a stable SBP-GP discretization. The results are generalized to the half-plane problem for the elastic wave equation in Section 3. Numerical examples are given in Section 4 and conclusions are given in Section 5.

2 The scalar wave equation in one space dimension

Consider the Cauchy problem for the one-dimensional scalar wave equation,

$$\begin{aligned} \rho\frac{\partial u}{\partial t^2} &= \frac{\partial}{\partial x}\left(\mu\frac{\partial u}{\partial x}\right) + f(x,t), \quad -\infty < x < \infty, \quad t \geq 0, \\ u(x,0) &= g_0(x), \quad u_t(x,0) = g_1(x), \quad -\infty < x < \infty. \end{aligned} \tag{2}$$

Here $\rho = \rho(x) > 0$ and $\mu = \mu(x) > 0$ are material coefficients that may vary in space, $g_0(x)$ and $g_1(x)$ are the initial data, and $f(x,t)$ is the external forcing function. The forcing and initial data are assumed to have compact support in the sub-domain $x \in \bar{\Omega}$ where $\bar{\Omega} = \{x_1 \leq x \leq x_2\}$. This is also assumed to be the domain of interest, i.e., where we want to find a numerical solution of (2).

We add a super-grid layer of width $\ell > 0$ on either side of $\bar{\Omega}$, and choose the coordinate system such that $x_1 - \ell = 0$ and $x_2 + \ell = x_{max}$. After introducing the coordinate mapping (1) (using the simplified notation $\phi = \phi^{(x)}$) and introducing an artificial dissipation of order $2p$, we obtain the modified wave equation

$$\rho\frac{\partial^2 v}{\partial t^2} = \phi\frac{\partial}{\partial \xi}\left(\phi\mu\frac{\partial v}{\partial \xi}\right) + \varepsilon\phi\frac{\partial^p}{\partial \xi^p}\left(\sigma\rho\frac{\partial^p v_t}{\partial \xi^p}\right) + f(X(\xi),t), \tag{3}$$

for $0 \leq \xi \leq x_{max}$ and $t \geq 0$, where ε is a constant. The solution of (3) is subject to the initial conditions

$$v(\xi,0) = g_0(X(\xi)), \quad v_t(\xi,0) = g_1(X(\xi)), \quad 0 \leq \xi \leq x_{max}. \tag{4}$$

The artificial dissipation is only added in the super-grid layers because the smooth function σ is constructed to satisfy

$$\sigma = \frac{1-\phi}{1-\varepsilon_L}.$$

Hence, $\sigma = 0$ where $\phi = 1$, i.e., for $x_1 \leq \xi \leq x_2$. Note the factor ρ in the artificial dissipation term in (3), which is used to make the relative strength of the dissipation independent of ρ.

We proceed by deriving an energy estimate. Note that the regular L_2 scalar product can be used to derive an energy estimate for the original wave equation (2). To estimate

the solution of (3) it is therefore natural to weigh the scalar product by the stretching function (1). For real-valued functions $v(\xi)$ and $w(\xi)$, we define

$$(v,w)_\phi = \int_0^{x_{max}} \frac{v(\xi)\,w(\xi)}{\phi}\,d\xi, \quad \|v\|_\phi^2 = (v,v)_\phi.$$

Note that $\|v\|_\phi$ is a norm of v because $\phi \geq \varepsilon_L > 0$.

Assume that $f = 0$ and multiply the differential equation (3) by v_t/ϕ and integrate over $0 \leq x \leq x_{max}$. After integration by parts, we get

$$(v_t, \rho v_{tt})_\phi + (v_{t\xi}, \phi^2 \mu v_\xi)_\phi = (-1)^p \varepsilon \left(\frac{\partial^p v_t}{\partial \xi^p}, \phi\sigma\rho \frac{\partial^p v_t}{\partial \xi^p} \right)_\phi + BT,$$

where the boundary term satisfies

$$BT = [v_t \phi \mu v_\xi]_0^{x_{max}} + \varepsilon \left[\left(v_t \frac{\partial^{p-1}}{\partial \xi^{p-1}} - v_{t\xi} \frac{\partial^{p-2}}{\partial \xi^{p-2}} + \ldots + (-1)^{p-1} \frac{\partial^{p-1} v_t}{\partial \xi^{p-1}} \right) \left(\sigma\rho \frac{\partial^p v_t}{\partial \xi^p} \right) \right]_0^{x_{max}}$$

The boundary term cancels if we impose p boundary conditions at $\xi = 0$ and $\xi = x_{max}$,

$$\begin{aligned} v(0,t) &= 0, \quad & v(x_{max},t) &= 0, \\ v_\xi(0,t) &= 0, \quad & v_\xi(x_{max},t) &= 0, \\ &\vdots & &\vdots & t \geq 0. \\ \frac{\partial^{p-1} v}{\partial \xi^{p-1}}(0,t) &= 0, \quad & \frac{\partial^{p-1} v}{\partial \xi^{p-1}}(x_{max},t) &= 0. \end{aligned} \tag{5}$$

We define the energy by $E(t) = \frac{1}{2}(v_t, \rho v_t)_\phi + \frac{1}{2}(\phi v_\xi, \phi\mu v_\xi)_\phi$, which is a norm of v because $\rho > 0$, $\mu > 0$, and $\phi \geq \varepsilon_L > 0$. We arrive at

$$\frac{d}{dt} E(t) = -\tilde{\varepsilon} \left(\frac{\partial^p v_t}{\partial \xi^p}, \phi\sigma\rho \frac{\partial^p v_t}{\partial \xi^p} \right)_\phi \leq 0, \quad \tilde{\varepsilon} := (-1)^{p-1}\varepsilon > 0.$$

Hence, $E(t) \leq E(0)$ for $t > 0$. We conclude that the initial boundary value problem (3), (4), (5) is well-posed if $\tilde{\varepsilon} \geq 0$. As we shall see below, for a fourth order accurate discretization of the wave equation, it is appropriate to either use a fourth ($p = 2$) or a sixth ($p = 3$) order artificial dissipation.

2.1 Discretizing the wave equation with super-grid layers

We discretize the one-dimensional spatial domain on the uniform grid $\xi_j = (j-1)h$, where j is an integer, $h > 0$ is the grid size and $\xi_{N_x} = x_{max}$. Time is discretized by $t_n = n\Delta_t$, where n is an integer and $\Delta_t > 0$ is the constant time step. A grid function is denoted $u_j^n = u(\xi_j, t_n)$. To simplify the notation, we occasionally drop the superscript or subscript on the grid function. We discretize the spatial operator in (3) by the formula

$$\frac{\partial}{\partial \xi} \left(\phi\mu \frac{\partial u}{\partial \xi} \right) \Big|_{\xi_j} = G(\phi\mu) u_j + \mathcal{O}(h^4),$$

which was derived in [16]. The difference formula is given by (here ϕ is absorbed into μ to simplify the notation),

$$G(\mu)u_j := \frac{1}{12h^2}\big(\bar{\mu}_{j-1}(u_j - u_{j-2}) - 16\bar{\mu}_{j-1/2}(u_j - u_{j-1}) \\ + 16\bar{\mu}_{j+1/2}(u_{j+1} - u_j) - \bar{\mu}_{j+1}(u_{j+2} - u_j)\big), \quad (6)$$

where μ is averaged according to

$$\bar{\mu}_j = \frac{1}{2}\left(3\mu_{j-1} - 4\mu_j + 3\mu_{j+1}\right), \quad (7)$$

$$\bar{\mu}_{j+1/2} = \frac{1}{8}\left(\mu_{j-1} + 3\mu_j + 3\mu_{j+1} + \mu_{j+2}\right). \quad (8)$$

A fourth order accurate time-integration scheme follows from the Taylor expansion

$$\frac{u_j^{n+1} - 2u_j^n + u_j^{n-1}}{\Delta_t^2} = u_{tt}|_j^n + \frac{\Delta_t^2}{12}u_{tttt}|_j^n + \mathcal{O}(\Delta_t^4).$$

We first consider the domain $x_1 \le \xi \le x_2$, where the artificial dissipation term is zero because $\sigma = 0$. In that case, the semi-discrete approximation of (3) gives the formula for the second time derivative of u_j,

$$\rho_j u_{tt}|_j = \phi_j G(\phi\mu)u_j + f(\xi_j, t). \quad (9)$$

An expression for the fourth time derivative of u_j follows by differentiating (9) twice,

$$\rho_j u_{tttt}|_j = \phi_j G(\phi\mu)u_{tt}|_j + f_{tt}(\xi_j, t). \quad (10)$$

Substituting (9) and (10) into the above Taylor series gives the fourth order time stepping scheme in the interior of the domain.

When a fourth order ($p = 2$) artificial dissipation term is used in (3), it is discretized according to

$$(\sigma\rho\, u_{\xi\xi t})_{\xi\xi}|_j \approx D_+D_-\left(\sigma_j\rho_j\, D_+D_-\frac{u_j^n - u_j^{n-1}}{\Delta_t}\right) =: Q_4(\sigma\rho)\left(\frac{u_j^n - u_j^{n-1}}{\Delta_t}\right). \quad (11)$$

By replacing D_+D_- by $(D_+D_-)^{p/2}$, this formula generalizes to artificial dissipations of order $2p$, for $p = 0, 2, 4, \ldots$.

A sixth order ($p = 3$) artificial dissipation term is discretized according to

$$(\sigma\rho\, u_{\xi\xi\xi t})_{\xi\xi\xi}|_j \approx D_+D_-D_+\left(\sigma_{j-1/2}\rho_{j-1/2}\, D_-D_+D_-\frac{u_j^n - u_j^{n-1}}{\Delta_t}\right) \\ =: Q_6(\sigma\rho)\left(\frac{u_j^n - u_j^{n-1}}{\Delta_t}\right), \quad (12)$$

where the average is used for the coefficient, e.g., $\sigma_{j-1/2} = (\sigma_j + \sigma_{j-1})/2$. The above formula can be generalized to any odd $p \ge 1$ by replacing the difference operator $D_+D_-D_+$ by $(D_+D_-)^{(p-1)/2}D_+$, and $D_-D_+D_-$ by $D_-(D_+D_-)^{(p-1)/2}$.

We arrive at the fully discrete approximation of (3),

$$\rho_j \frac{u_j^{n+1} - 2u_j^n + u_j^{n-1}}{\Delta_t^2} = \phi_j G(\phi\mu) u_j^n + f(\xi_j, t_n) + \frac{\Delta_t^2}{12}\left(\phi_j G(\phi\mu)\ddot{u}_j^n + f_{tt}(\xi_j, t_n)\right) + \varepsilon\phi_j Q_{2p}(\sigma\rho)\left(\frac{u_j^n - u_j^{n-1}}{\Delta_t}\right). \quad (13)$$

Here $\ddot{u}_j^n = (\phi_j G(\phi\mu)u_j^n + f(\xi_j, t_n))/\rho_j$. The stencil for $G(\phi\mu)u_j$ is five points wide. If a 4th order dissipation is used, which also is five points wide, we must provide boundary conditions at two ghost points. Three ghost points are needed if a sixth order dissipation is used, because its stencil is seven points wide. In general, we need $\max(2, p)$ boundary conditions.

A natural discretization of the boundary conditions (5) is given by

$$B_{sg}(u^n) = 0, \quad B_{sg}(\ddot{u}^n) = 0, \quad n = 0, 1, 2, \ldots, \quad (14)$$

where the boundary operator $B_{sg}(u)$ picks out $\tilde{p} = \max(2, p)$ ghost point values outside each boundary,

$$B_{sg}(u) = (u_{1-\tilde{p}}, \ldots, u_0, u_{N_x+1}, \ldots, u_{N_x+\tilde{p}})^T, \quad \tilde{p} = \max(2, p). \quad (15)$$

Remark 1. *The implementation of the time-stepping scheme* (13), (14) *can be simplified by writing it in predictor-corrector form, see [16] for details.*

2.2 Discrete energy estimate

We begin by defining the one-dimensional discrete L_2 scalar product and norm for real-valued grid functions v_j, w_j, by

$$(v, w)_{h1} = h\sum_{j=1}^{N_x} v_j w_j, \quad \|v\|_{h1}^2 = (v, v)_{h1}.$$

The SBP property of $G(\phi\mu)u_j$ is specified in the following lemma.

Lemma 1. *Let u and v be real-valued grid functions satisfying the boundary condition $B_{sg}(u) = 0$, $B_{sg}(v) = 0$, and let $\mu_j > 0$ and $\phi_j \geq \varepsilon_L > 0$ be the grid functions representing the material property and the stretching function, respectively. The spatial operator $G(\phi\mu)$, defined by* (6)*, satisfies*

$$(v, Gu)_{h1} = -K_0(v, u) \in \Re, \quad (16)$$

where the function $K_0(v, u)$ is bilinear, symmetric and positive definite, i.e., $K_0(v, u) = K_0(u, v)$ and $K_0(u, u) \geq \gamma\|u\|_{h1}^2$, $\gamma > 0$.

Proof. See Appendix B.1. □

The artificial dissipation term satisfies a similar lemma.

Lemma 2. *Let the real-valued grid functions σ and ρ satisfy $\sigma_j \geq 0$ and $\rho_j > 0$. Furthermore, let u and v be real-valued grid functions that satisfy the boundary conditions $B_{sg}(u) = 0$ and $B_{sg}(v) = 0$. The artificial dissipation operator $Q_{2p}(\sigma\rho)$, defined by* (11) *or* (12)*, satisfies*

$$(v, Q_{2p}u)_{h1} = (-1)^p C_0(v, u) \in \Re,$$

where the function $C_0(v, u)$ is bilinear, symmetric, and positive semi-definite, i.e., $C_0(v, u) = C_0(u, v)$ and $C_0(u, u) \geq 0$.

Proof. See Appendix B.2. □

To derive a discrete energy estimate for (13), it is convenient to work with grid functions that do not have ghost points. We therefore define grid functions $\bar{u}_j$ and $\bar{v}_j$ such that

$$\bar{u}_j = u_j, \quad \bar{v}_j = v_j, \quad 1 \leq j \leq N_x.$$

We also define square matrices K and C_{2p} such that,

$$K_0(u, v) = (\bar{u}, K\bar{v})_{h1}, \quad C_0(u, v) = (\bar{u}, C_{2p}\bar{v})_{h1}, \quad \text{if } B_{sg}(u) = 0 \text{ and } B_{sg}(v) = 0.$$

Because the function $K_0(u, v)$ is symmetric and positive definite, $(\bar{u}, K\bar{v})_{h1} = (K\bar{u}, \bar{v})_{h1}$ and $(\bar{v}, K\bar{v})_{h1} > 0$ for all $\bar{v} \neq 0$, i.e. $K = K^T$ and $K > 0$. From (16) we have $(u, Gv)_{h1} = -(\bar{u}, K\bar{v})_{h1}$. By taking $u = 0$ except at one interior grid point where $u_j = 1$, we obtain a pointwise identity. The same procedure applies to the damping term Q_{2p}, and we conclude that

$$Gv = -K\bar{v} \quad \text{and} \quad Q_{2p}v = (-1)^p C_{2p}\bar{v}, \quad \text{if } B_{sg}(v) = 0. \tag{17}$$

We write the forcing in (13) in vector form as $F(t)$, with elements $F_j(t) = f(X(\xi_j), t)$, $j = 1, 2, \ldots, N_x$. Also introduce the diagonal matrices M and Φ with elements $M_{jj} = \tilde{\rho}_j$ and $\Phi_{jj} = \phi_j$, respectively. Because the acceleration satisfies the boundary conditions $B_{sg}(\ddot{u}) = 0$, there is a grid function without ghost points with elements $\ddot{\bar{u}}_j = \ddot{u}_j$, for $1 \leq j \leq N_x$, such that

$$\ddot{\bar{u}} = -M^{-1}\Phi K\bar{u} + M^{-1}F.$$

We summarize these results in the following Lemma.

Lemma 3. *The time-integration scheme* (13) *can be written in matrix form as*

$$\frac{1}{\Delta_t^2} M\left(\bar{u}^{n+1} - 2\bar{u}^n + \bar{u}^{n-1}\right) = -\Phi K\bar{u}^n + F(t^n) + \frac{\Delta_t^2}{12}\left(-\Phi K\ddot{\bar{u}}^n + F_{tt}(t_n)\right) - \frac{\tilde{\varepsilon}}{\Delta_t}\Phi C_{2p}\left(\bar{u}^n - \bar{u}^{n-1}\right), \quad n = 0, 1, 2, \ldots, \tag{18}$$

where $\tilde{\varepsilon} = (-1)^{p-1}\varepsilon$. The matrices K and C_{2p}, defined by (17)*, are both symmetric; K is positive definite and C_{2p} is positive semi-definite. The matrices M and Φ are diagonal with positive elements. The solution of* (18) *is subject to the inital conditions*

$$\bar{u}_j^0 = g_0(X(\xi_j)), \quad \bar{u}_j^{-1} = \tilde{g}_1(X(\xi_j)), \quad j = 1, 2, \ldots, N_x, \tag{19}$$

where $\tilde{g}_1$ depends on g_0 and g_1.

Our main result for the SBP discretization of the one-dimensional wave equation with super-grid layers is formulated in the following theorem.

Theorem 1. *Let $\bar{u}^n$, $n = 0, 1, 2, \ldots$, be a solution of the time-integration scheme described in Lemma 3. Define the discrete energy by*

$$e^{n+1/2} := \frac{1}{\Delta_t^2}\left(\bar{u}^{n+1} - \bar{u}^n, \Phi^{-1}M(\bar{u}^{n+1} - \bar{u}^n)\right)_{h1} + \left(\bar{u}^{n+1}, K\bar{u}^n - \frac{\Delta_t^2}{12}KM^{-1}\Phi K\bar{u}^n\right)_{h1} - \frac{\tilde{\varepsilon}}{2\Delta_t}\left(\bar{u}^{n+1} - \bar{u}^n, C_{2p}\left(\bar{u}^{n+1} - \bar{u}^n\right)\right)_{h1}. \quad (20)$$

The discrete energy $e^{n+1/2}$ is a norm of the solution if the inequalities

$$2\left(\bar{w}, \Phi^{-1}MR_1\bar{w}\right)_{h1} > \tilde{\varepsilon}\Delta_t\left(\bar{w}, C_{2p}\bar{w}\right)_{h1}, \quad (21)$$

$$\left(\bar{w}, \Phi^{-1}MR_2\bar{w}\right)_{h1} > 0, \quad (22)$$

are satisfied for all vectors $\bar{w} \neq 0$. Here, $R_1 = P_1(\Delta_t^2 M^{-1}\Phi K)$ and $R_2 = P_2(\Delta_t^2 M^{-1}\Phi K)$, where P_1 and P_2 are the matrix polynomials,

$$P_1(A) := I - \frac{1}{4}A + \frac{1}{48}A^2, \quad P_2(A) := \frac{1}{4}A - \frac{1}{48}A^2. \quad (23)$$

If $\tilde{\varepsilon} := (-1)^{p-1}\varepsilon \geq 0$ and $F(t) = 0$, the solution of (18) satisfies the energy estimate

$$e^{n+1/2} = e^{n-1/2} - \frac{\tilde{\varepsilon}}{2\Delta_t}\left(\bar{u}^{n+1} - \bar{u}^{n-1}, C_{2p}\left(\bar{u}^{n+1} - \bar{u}^{n-1}\right)\right)_{h1}, \quad (24)$$

which is non-increasing in n. The time-stepping scheme (18) is therefore stable if the time step satisfies the inequalities (21) and (22).

Proof. Assuming $F(t) = 0$, we derive an energy estimate for (18) by forming the scalar product between $(\bar{u}^{n+1} - \bar{u}^{n-1})\Phi^{-1}$ and (18) (note that Φ is non-singular because $\phi_j \geq \varepsilon_L > 0$). For the left hand side, we get

$$\frac{1}{\Delta_t^2}\left(\bar{u}^{n+1} - \bar{u}^{n-1}, \Phi^{-1}M(\bar{u}^{n+1} - 2\bar{u}^n + \bar{u}^{n-1})\right)_{h1} = \frac{1}{\Delta_t^2}\left(\bar{u}^{n+1} - \bar{u}^n, \Phi^{-1}M(\bar{u}^{n+1} - \bar{u}^n)\right)_{h1} - \frac{1}{\Delta_t^2}\left(\bar{u}^n - \bar{u}^{n-1}, \Phi^{-1}M(\bar{u}^n - \bar{u}^{n-1})\right)_{h1}. \quad (25)$$

Because the matrices K, Φ, and M are symmetric, the first two terms on the right hand side of (18) become

$$\left(\bar{u}^{n+1} - \bar{u}^{n-1}, -K\bar{u}^n + \frac{\Delta_t^2}{12}KM^{-1}\Phi K\bar{u}^n\right)_{h1} = \left(\bar{u}^{n+1}, -K\bar{u}^n + \frac{\Delta_t^2}{12}KM^{-1}\Phi K\bar{u}^n\right)_{h1} - \left(\bar{u}^n, -K\bar{u}^{n-1} + \frac{\Delta_t^2}{12}KM^{-1}\Phi K\bar{u}^{n-1}\right)_{h1}, \quad (26)$$

where we have used $\Phi M^{-1} = M^{-1}\Phi$.

To analyze the dissipative term (last term on the right hand side of (18)), it is helpful to first consider an expression of the type $(\bar{x} + \bar{y}, C\bar{y})_{h1}$, where $C = C_{2p}$. We have

$$(\bar{x} + \bar{y}, C\bar{y})_{h1} = (\bar{x} + \bar{y}, C(\bar{x} + \bar{y}))_{h1} - (\bar{x} + \bar{y}, C\bar{x})_{h1}.$$

Also, $(\bar{x}+\bar{y}, C\bar{y})_{h1} = (\bar{x}, C\bar{y})_{h1} + (\bar{y}, C\bar{y})_{h1}$. Because C is symmetric,

$$(\bar{x}+\bar{y}, C\bar{y})_{h1} = \frac{1}{2}(\bar{x}+\bar{y}, C(\bar{x}+\bar{y}))_{h1} - \frac{1}{2}(\bar{x}+\bar{y}, C\bar{x})_{h1} + \frac{1}{2}(\bar{x}, C\bar{y})_{h1} + \frac{1}{2}(\bar{y}, C\bar{y})_{h1} = \frac{1}{2}(\bar{x}+\bar{y}, C(\bar{x}+\bar{y}))_{h1} - \frac{1}{2}(\bar{x}, C\bar{x})_{h1} + \frac{1}{2}(\bar{y}, C\bar{y})_{h1}.$$

Now take $\bar{x} = \bar{u}^{n+1} - \bar{u}^n$ and $\bar{y} = \bar{u}^n - \bar{u}^{n-1}$. The expression for the dissipative term in (17) becomes

$$\left(\bar{u}^{n+1} - \bar{u}^{n-1}, C_{2p}\left(\bar{u}^n - \bar{u}^{n-1}\right)\right)_{h1} = \frac{1}{2}\left(\bar{u}^{n+1} - \bar{u}^{n-1}, C_{2p}\left(\bar{u}^{n+1} - \bar{u}^{n-1}\right)\right)_{h1} - \frac{1}{2}\left(\bar{u}^{n+1} - \bar{u}^{n}, C_{2p}\left(\bar{u}^{n+1} - \bar{u}^{n}\right)\right)_{h1} + \frac{1}{2}\left(\bar{u}^{n} - \bar{u}^{n-1}, C_{2p}\left(\bar{u}^{n} - \bar{u}^{n-1}\right)\right)_{h1}. \quad (27)$$

By inspection of the three terms (25), (26), and (27), it is natural to define the discrete energy according to (20). After re-arranging the terms of (25), (26), and (27), we arrive at the energy estimate (24).

To analyze the properties of $e^{n+1/2}$, we re-write the terms of (20) that involve K. Because K is symmetric,

$$(\bar{u}^{n+1}, K\bar{u}^n)_{h1} = \frac{1}{4}(\bar{u}^{n+1} + \bar{u}^n, K(\bar{u}^{n+1} + \bar{u}^n))_{h1} - \frac{1}{4}(\bar{u}^{n+1} - \bar{u}^n, K(\bar{u}^{n+1} - \bar{u}^n))_{h1}.$$

The same procedure applies to the terms involving the matrix $KM^{-1}\Phi K$, which also is symmetric because $\Phi M^{-1} = M^{-1}\Phi$. The discrete energy $e^{n+1/2}$ can therefore be grouped into two terms

$$e^{n+1/2} = \left(\bar{u}^{n+1} - \bar{u}^n, \left(\frac{1}{\Delta_t^2}\Phi^{-1}M - \frac{1}{4}K + \frac{\Delta_t^2}{48}KM^{-1}\Phi K + \frac{\varepsilon(-1)^p}{2\Delta_t}C_{2p}\right)(\bar{u}^{n+1} - \bar{u}^n)\right)_{h1} + \left(\bar{u}^{n+1} + \bar{u}^n, \left(\frac{1}{4}K - \frac{\Delta_t^2}{48}KM^{-1}\Phi K\right)(\bar{u}^{n+1} + \bar{u}^n)\right)_{h1}.$$

We have $e^{n+1/2} > 0$ if both terms are positive. By taking $\bar{w} = \bar{u}^{n+1} - \bar{u}^n$, we see that the first term is positive if (21) is satisfied. Setting $\bar{w} = \bar{u}^{n+1} + \bar{u}^n$ shows that the second term is positive if (22) is satisfied. This completes the proof. □

Remark 2. *In [16] we used the Cayley-Hamilton theorem to analyze the stability of the non-dissipative version of the time-stepping scheme* (18)*. When* $\varepsilon = 0$ *the inequalities* (21) *and* (22) *simplify to eigenvalue conditions, and one can prove that the scheme is stable under the time step restriction*

$$\Delta_t \leq \frac{2\sqrt{3}}{\max_j \sqrt{\kappa_j}}, \quad M^{-1}\Phi K\mathbf{e}_j = \kappa_j \mathbf{e}_j, \quad \varepsilon = 0.$$

Note that $M^{-1}\Phi K$ *has the same spectrum as the symmetric positive definite matrix*

$$M^{-1/2}\Phi^{1/2}K\Phi^{1/2}M^{-1/2}.$$

Hence all eigenvalues κ_j *are real and positive.*

Unfortunately, the energy estimate does not tell us how large the eigenvalues are, and therefore only says that the time-stepping scheme is stable if the time-step is sufficiently small.

2.3 Estimating the time step

In this section we perform a von Neumann analysis to estimate the stability limit of the time step. For this purpose, we assume constant stretching and dissipation coefficients, as well as constant material properties,

$$\sigma = \sigma_0 \geq 0, \quad \phi = \phi_0 \geq \varepsilon_L > 0, \quad \mu = \mu_0 > 0, \quad \rho = \rho_0 > 0.$$

To study the stability we assume that the external forcing is zero, $f(x,t) = 0$. When all coefficients are constant, the fully discrete scheme (13) simplifies to

$$u_j^{n+1} - 2u_j^n + u_j^{n-1} = \frac{\Delta_t^2 \phi_0^2 \mu_0}{\rho_0} \left(D_4 u_j^n + \frac{\Delta_t^2 \phi_0^2 \mu_0}{12\rho_0} (D_4)^2 u_j^n \right) + \varepsilon \sigma_0 \phi_0 \Delta_t \left(D_+ D_- \right)^p \left(u_j^n - u_j^{n-1} \right), \quad (28)$$

where $D_4 u_j = D_+ D_- u_j - \frac{h^2}{12} (D_+ D_-)^2 u_j$ is a fourth order accurate approximation of $u_{\xi\xi}$. We replace the boundary conditions by the assumption that the solution is 2π-periodic in space, and expand the solution in a Fourier series (for notational simplicity, we assume that N_x is even),

$$u_j^n = \sum_{k=1-N_x/2}^{N_x/2} \hat{u}^n(k) e^{ikx_j}, \quad N_x \text{ even}.$$

The spatial difference operators in (28) correspond to the Fourier symbols

$$D_4 u_j \to -\frac{1}{h^2} \left(4 \sin^2 \frac{kh}{2} + \frac{4}{3} \sin^4 \frac{kh}{2} \right) \hat{u}(k) =: -\frac{\hat{\psi}(k)}{h^2} \hat{u}(k), \quad (29)$$

$$\left(D_+ D_- \right)^p u_j \to (-1)^p \frac{4^p}{h^{2p}} \sin^{2p} \left(\frac{kh}{2} \right) \hat{u}(k). \quad (30)$$

On the Fourier side, (28) corresponds to the difference equation with constant coefficients

$$\hat{u}^{n+1} - 2\hat{u}^n + \hat{u}^{n-1} = -2\alpha \hat{u}^n - 2\delta \left(\hat{u}^n - \hat{u}^{n-1} \right), \quad (31)$$

where

$$2\alpha = \frac{\Delta_t^2 \mu_0 \phi_0^2 \hat{\psi}}{h^2 \rho_0} \left(1 - \frac{1}{12} \frac{\Delta_t^2 \mu_0 \phi_0^2 \hat{\psi}}{h^2 \rho_0} \right), \quad 2\delta = \tilde{\varepsilon} \sigma_0 \phi_0 \Delta_t \frac{4^p}{h^{2p}} \sin^{2p} \left(\frac{kh}{2} \right). \quad (32)$$

As before, $\tilde{\varepsilon} = \varepsilon(-1)^{p-1}$. Note that both α and δ are real.

We solve (31) using the ansatz $\hat{u}^n = \kappa^n \hat{u}^0$. There are nontrivial solutions if and only if the characteristic equation

$$\kappa^2 - 2\kappa + 1 = -2\alpha\kappa - 2\delta(\kappa - 1), \quad (33)$$

is satisfied. A solution of the difference equation (31) is unstable if there is a root of (33) with $|\kappa| > 1$. A necessary condition for stability is therefore $|\kappa| \leq 1$.

Away from the super-grid layers, we have $\sigma(x) = 0$, corresponding to $\sigma_0 = 0$ and $\delta = 0$. We therefore start by analyzing the case $\delta = 0$. Thereafter, we consider $\delta > 0$, corresponding to $\tilde{\varepsilon}\sigma_0\phi_0 > 0$.

2.3.1 The case $\delta = 0$.

The case $\sigma = 0$ corresponds to $\phi = 1$, and we assume $\phi_0 = 1$ in the following. The characteristic equation (33) has the solutions

$$\kappa_{1,2} = 1 - \alpha \pm \sqrt{-2\alpha + \alpha^2}.$$

The discriminant, $\alpha^2 - 2\alpha = \alpha(\alpha - 2)$ is positive if $\alpha > 2$ or $\alpha < 0$. When $\alpha > 2$, $\kappa_2 = 1 - \alpha - \sqrt{\alpha(\alpha - 2)} < -1$, and when $\alpha < 0$, $\kappa_1 = 1 + |\alpha| + \sqrt{|\alpha|(2 + |\alpha|)} > 1$. We conclude that the difference equation (31) has unstable solutions if $\alpha > 2$ or $\alpha < 0$.

The discriminant is negative or zero for $0 \leq \alpha \leq 2$. Then the roots of (33) are complex conjugated,

$$\kappa_{1,2} = 1 - \alpha \pm i\sqrt{2\alpha - \alpha^2}.$$

The magnitude of the roots satisfy

$$|\kappa_{1,2}|^2 = (1 - \alpha)^2 + (2\alpha - \alpha^2) = 1,$$

and we conclude that the necessary condition for stability is satisfied.

We proceed by analyzing the time step corresponding to $0 \leq \alpha \leq 2$. From (32) (with $\phi_0 = 1$) we have

$$2\alpha = \xi - \frac{\xi^2}{12}, \quad \xi = \frac{\Delta_t^2 \mu_0 \hat{\psi}}{h^2 \rho_0}. \tag{34}$$

Therefore, $\alpha \leq 2$ if $\xi - \xi^2/12 \leq 4$. However, this inequality is always satisfied because

$$\xi - \frac{\xi^2}{12} \leq 3,$$

for all real ξ. The condition $\alpha \geq 0$ is satisfied if $\xi - \xi^2/12 \geq 0$, which is equivalent to

$$p(\xi) \geq 0, \quad p(\xi) = \frac{\xi}{4} - \frac{\xi^2}{48}.$$

The equation $p(\xi) = 0$ has the solutions $\xi = 0$ and $\xi = 12$, and it is easy to verify that $p(\xi) > 0$ for $0 < \xi < 12$.

We next study how ξ depends on the parameters in (34). The Fourier symbol $\hat{\psi}$, defined by (29), satisfies

$$0 \leq \hat{\psi}(k) \leq \frac{16}{3},$$

where the max value is attained for $kh = \pi$. This wave number corresponds to the wave length $2h$, i.e., 2 grid points per wave length, which is the shortest wave that can be represented on the grid. Since $\Delta_t^2 \mu_0 \hat{\psi} \geq 0$ and $h^2 \rho_0 > 0$, we have

$$\xi \leq \frac{\Delta_t^2 \mu_0}{h^2 \rho_0} \frac{16}{3}.$$

Therefore, $0 \leq \xi \leq 12$ corresponds to the time step restriction

$$0 \leq \frac{\Delta_t}{h} \sqrt{\frac{\mu_0}{\rho_0}} \leq \frac{3}{2}.$$

As expected, the time step is governed by the largest local phase velocity, c_{max}, and we arrive at

$$\frac{\Delta_t}{h} \leq \frac{3}{2c_{max}}, \quad c_{max} = \max_{x_1 \leq \xi \leq x_2} \sqrt{\frac{\mu(\xi)}{\rho(\xi)}}. \tag{35}$$

2.3.2 The case $\delta > 0$.

For simplicity we assume that $\alpha = 0$. When $\alpha = 0$ and $\delta > 0$, the characteristic equation (33) is solved by

$$\kappa_{1,2} = 1 - \delta \pm \sqrt{\delta^2} = 1 - \delta \pm \delta.$$

Hence, $\kappa_1 = 1$ and $\kappa_2 = 1 - 2\delta$. The necessary condition for stability is therefore satisfied when $|\kappa_2| \leq 1$, which corresponds to $-1 \leq 1 - 2\delta \leq 1$, i.e., $0 \leq \delta \leq 1$. The definition (32) gives

$$\delta = \tilde{\varepsilon}\sigma_0\phi_0 \frac{4^p \Delta_t}{2h^{2p}} \sin^{2p}\left(\frac{kh}{2}\right),$$

which attains its maxima when $kh = \pi$ and $\sigma_0\phi_0 \approx 1/4$, because $\sigma \approx 1 - \phi$ when $\varepsilon_L \ll 1$. Therefore,

$$0 \leq \delta \leq \tilde{\varepsilon}\frac{4^p \Delta_t}{8h^{2p}} \leq 1, \quad \Rightarrow \quad 0 \leq \frac{\Delta_t}{h} \leq \frac{8h^{2p-1}}{4^p \tilde{\varepsilon}}.$$

We want the dissipation coefficient $\tilde{\varepsilon}$ to be as large as possible without restricting the time step beyond the limit for the case $\delta = 0$, which is given by (35). We must therefore take

$$\frac{8h^{2p-1}}{4^p \tilde{\varepsilon}} \geq \frac{3}{2c_{max}}, \quad \Rightarrow \quad \tilde{\varepsilon} \leq \frac{16}{3}\frac{c_{max} h^{2p-1}}{4^p}.$$

If we determine the time step by the formula $\Delta_t/h = C_{cfl}/c_{max}$, where C_{cfl} is a constant, we can write $c_{max} = hC_{cfl}/\Delta_t$. It is also convenient to scale the dissipation coefficient so that it becomes independent of h and Δ_t. We conclude that the necessary condition for stability for the case ($\delta > 0,\ \alpha = 0$) are satisfied if

$$\tilde{\varepsilon} = \gamma_{2p}\frac{h^{2p}}{\Delta_t}, \quad \gamma_{2p} \leq \frac{16\, C_{cfl}}{3 \cdot 4^p}.$$

3 The elastic wave equation

This section analyses the elastic wave equations with super-grid layers, and describes a fourth order accurate discretization based on SBP-GP operators. For clarity of presentation, the description and analysis is done in two space dimensions. It should be straightforward for the reader to generalize the results to the three-dimensional equations.

Consider the time-dependent elastic wave equation in the two-dimensional half-plane $\mathbf{x} = (x, y) \in \Omega = \{-\infty < x < \infty,\ 0 \leq y \leq \infty\}$, governing the displacement with Cartesian components $\mathbf{u} = (u, v)^T$,

$$\begin{aligned} \rho u_{tt} &= ((2\mu + \lambda)u_x + \lambda v_y)_x + (\mu v_x + \mu u_y)_y + f^{(x)}, \\ \rho v_{tt} &= (\mu v_x + \mu u_y)_x + (\lambda u_x + (2\mu + \lambda)v_y)_y + f^{(y)}, \end{aligned} \quad \mathbf{x} \in \Omega,\ t \geq 0. \tag{36}$$

The heterogeneous isotropic material is characterized by the density $\rho(\mathbf{x}) > 0$, and the Lamé parameters $\lambda(\mathbf{x})$ and $\mu(\mathbf{x}) > 0$. In the following we assume $\lambda(\mathbf{x}) > 0$. Furthermore, $(f^{(x)}, f^{(y)})^T$ are the components of the external forcing functions. The displacement is subject to initial conditions

$$\mathbf{u} = \mathbf{g}_0, \quad \mathbf{u}_t = \mathbf{g}_1, \quad \mathbf{x} \in \Omega,\ t = 0, \tag{37}$$

where $\mathbf{g}_0$ and $\mathbf{g}_1$ are the initial data. The solution is subject to a normal stress condition on the physical boundary,

$$\begin{aligned} \mu(v_x + u_y) &= \tau^{(xy)}, \\ (2\mu+\lambda)v_y + \lambda u_x &= \tau^{(yy)}, \end{aligned} \qquad -\infty < x < \infty,\ y = 0,\ t \geq 0, \tag{38}$$

where $\tau^{(yy)}$ and $\tau^{(xy)}$ are the boundary forcing functions. When $\tau^{(yy)} = \tau^{(xy)} = 0$ this boundary condition is often called a free surface, or traction free, condition.

Similar to the one-dimensional case, we assume that we want to calculate the solution of (36)-(38) in the sub-domain $\mathbf{x} \in \bar{\Omega} = \{x_1 \leq x \leq x_2,\ 0 \leq y \leq y_2\}$, and that the initial data, external forcing, and boundary forcing functions have compact support in $\bar{\Omega}$. We add super-grid layers of thickness ℓ outside all sides of $\bar{\Omega}$, except $y = 0$. We choose the coordinate system such that $x_1 - \ell = 0$, $x_2 + \ell = x_{max}$, $y_2 + \ell = y_{max}$, and introduce the coordinate transformation (1). Because of the physical boundary condition (38) at $y = 0$, we use a stretching function in the η-direction that satisfies $\phi^{(y)} = 1$ for $0 \leq \eta \leq y_2$. Similar to the one-dimensional case, $\phi^{(x)} = 1$ for $x_1 \leq \xi \leq x_2$. See Figure 2 for a layout of this configuration.

After transforming the spatial derivatives in (36) and adding an artificial dissipation of order $2p$, we get the elastic wave equation with super-grid layers,

$$\begin{aligned} \rho u_{tt} = \phi^{(x)}\frac{\partial}{\partial\xi}\left(\phi^{(x)}(2\mu+\lambda)u_\xi + \phi^{(y)}\lambda v_\eta\right) + \phi^{(y)}\frac{\partial}{\partial\eta}\left(\phi^{(x)}\mu v_\xi + \phi^{(y)}\mu u_\eta\right) + \\ \epsilon\phi^{(x)}\frac{\partial^p}{\partial\xi^p}\left(\sigma^{(x)}\rho\frac{\partial^p u_t}{\partial\xi^p}\right) + \epsilon\phi^{(y)}\frac{\partial^p}{\partial\eta^p}\left(\sigma^{(y)}\rho\frac{\partial^p u_t}{\partial\eta^p}\right) + f^{(x)}, \end{aligned} \tag{39}$$

$$\begin{aligned} \rho v_{tt} = \phi^{(x)}\frac{\partial}{\partial\xi}\left(\phi^{(x)}\mu v_\xi + \phi^{(y)}\mu u_\eta\right) + \phi^{(y)}\frac{\partial}{\partial\eta}\left(\phi^{(x)}\lambda u_\xi + \phi^{(y)}(2\mu+\lambda)v_\eta\right) + \\ \epsilon\phi^{(x)}\frac{\partial^p}{\partial\xi^p}\left(\sigma^{(x)}\rho\frac{\partial^p v_t}{\partial\xi^p}\right) + \epsilon\phi^{(y)}\frac{\partial^p}{\partial\eta^p}\left(\sigma^{(y)}\rho\frac{\partial^p v_t}{\partial\eta^p}\right) + f^{(y)}. \end{aligned} \tag{40}$$

Similar to the one-dimensional case, the coefficients in the damping terms are related to the mapping functions through

$$\sigma^{(x)} = \frac{1-\phi^{(x)}}{1-\varepsilon_L}, \quad \sigma^{(y)} = \frac{1-\phi^{(y)}}{1-\varepsilon_L}.$$

The damping in the ξ-direction is therefore only added in the layers $0 \leq \xi \leq \ell = x_1$, $x_2 \leq \xi \leq x_2 + \ell = x_{max}$. In the η-direction, the damping is only added in the layer $y_2 \leq \eta \leq y_2 + \ell = y_{max}$. In particular, note that there is no damping in the η-direction near the physical boundary.

The normal stress boundary conditions (38) are also mapped to computational coordinates using (1). Because $\phi^{(y)} = 1$ for $y = \eta = 0$, we get

$$\begin{aligned} \mu\left(\phi^{(x)}v_\xi + u_\eta\right) &= \tau^{(xy)}, \\ (2\mu+\lambda)v_\eta + \lambda\phi^{(x)}u_\xi &= \tau^{(yy)}, \end{aligned} \qquad 0 \leq \xi \leq x_{max},\ \eta = 0,\ t \geq 0, \tag{41}$$

We proceed by deriving an energy estimate for the solution of (39), (40), (41). Because $\phi^{(x)} \geq \varepsilon_L > 0$ and $\phi^{(y)} \geq \varepsilon_L > 0$, we can define a weighted scalar product and norm for real-valued functions u and v by

$$(u,v)_{2\phi} = \int_0^{y_{max}} \int_0^{x_{max}} \frac{u(\xi,\eta)\, v(\xi,\eta)}{\phi^{(x)}(\xi)\, \phi^{(y)}(\eta)}\, d\xi d\eta, \quad \|u\|_{2\phi}^2 = (u,u)_{2\phi}.$$

Consider the case without external and boundary forcing, i.e. $f^{(x)} = 0$, $f^{(y)} = 0$, $\tau^{(xy)} = 0$ and $\tau^{(yy)} = 0$. The energy estimate is derived by multiplying (39) by $u_t/(\phi^{(x)}\phi^{(y)})$, and (40) by $v_t/(\phi^{(x)}\phi^{(y)})$. We then add the results together and integrate over the computational domain. After integration by parts we obtain

$$\frac{d}{dt}E_2(t) = -\tilde{\varepsilon}\left(\phi^{(x)}\frac{\partial^p u_t}{\partial \xi^p}, \sigma^{(x)}\rho\frac{\partial^p u_t}{\partial \xi^p}\right)_{2\phi} - \tilde{\varepsilon}\left(\phi^{(x)}\frac{\partial^p v_t}{\partial \xi^p}, \sigma^{(x)}\rho\frac{\partial^p v_t}{\partial \xi^p}\right)_{2\phi} - \tilde{\varepsilon}\left(\phi^{(y)}\frac{\partial^p u_t}{\partial \eta^p}, \sigma^{(y)}\rho\frac{\partial^p u_t}{\partial \eta^p}\right)_{2\phi} - \tilde{\varepsilon}\left(\phi^{(y)}\frac{\partial^p v_t}{\partial \eta^p}, \sigma^{(y)}\rho\frac{\partial^p v_t}{\partial \eta^p}\right)_{2\phi} + BT_2. \quad (42)$$

In the stretched coordinates, the elastic energy satisfies

$$2E_2(t) = (u_t, \rho u_t)_{2\phi} + (v_t, \rho v_t)_{2\phi} + \left(\phi^{(x)}u_\xi + \phi^{(y)}v_\eta, \lambda\left(\phi^{(x)}u_\xi + \phi^{(y)}v_\eta\right)\right)_{2\phi} + \left(\phi^{(x)}v_\xi + \phi^{(y)}u_\eta, \mu\left(\phi^{(x)}v_\xi + \phi^{(y)}u_\eta\right)\right)_{2\phi} + 2\left(\phi^{(x)}u_\xi, \mu\phi^{(x)}u_\xi\right)_{2\phi} + 2\left(\phi^{(y)}v_\eta, \mu\phi^{(y)}v_\eta\right)_{2\phi}. \quad (43)$$

The boundary term in (42) can be evaluated in the same way as in the one-dimensional case, given in (2). Because $\tau^{(xy)} = \tau^{(yy)} = 0$ in boundary condition (41), all boundary terms from $\eta = 0$ cancel. The remaining boundary terms in BT_2 become zero if we enforce the boundary conditions

$$\mathbf{u} = 0, \quad \mathbf{u}_\xi = 0, \cdots, \quad \frac{\partial^{p-1}\mathbf{u}}{\partial \xi^{p-1}} = 0, \quad \xi = \{0,\ x_{max}\},\ 0 \leq \eta \leq y_{max},\ t \geq 0, \quad (44)$$

and

$$\mathbf{u} = 0, \quad \mathbf{u}_\eta = 0, \cdots, \quad \frac{\partial^{p-1}\mathbf{u}}{\partial \eta^{p-1}} = 0, \quad 0 \leq \xi \leq x_{max},\ \eta = y_{max},\ t \geq 0. \quad (45)$$

The elastic energy $E_2(t)$ is a norm of $\mathbf{u}$ for all $\mathbf{u}$ that satisfy the homogeneous boundary conditions (41), (44), and (45), because $\rho > 0$, $\lambda > 0$, $\mu > 0$, $\phi^{(x)} \geq \varepsilon_L$, and $\phi^{(y)} \geq \varepsilon_L$, where $\varepsilon_L > 0$. Note that the boundary conditions (44) and (45) remove the translational and rotational rigid body invariants from $\mathbf{u}$. These invariants would otherwise correspond to motions with zero elastic energy and make $E_2(t)$ a semi-norm, see e.g. [16] for details.

We summarize the results of this section in the following lemma.

Lemma 4. *Let $\mathbf{u} = (u, v)$ be a solution of the elastic wave equation with super-grid layers (39), (40), subject to the boundary conditions (41), (44), (45). Let the order of the artificial dissipation be $2p$, $p \geq 0$. Furthermore, assume that the external and boundary forcing functions are zero, i.e. $f^{(x)} = f^{(y)} = 0$ and $\tau^{(xy)} = \tau^{(yy)} = 0$. Also, assume that the material parameters and the stretching functions satisfy $\lambda > 0$, $\mu > 0$, $\rho > 0$, $\phi^{(x)} \geq \varepsilon_L$, and $\phi^{(y)} \geq \varepsilon_L$, where $\varepsilon_L > 0$. Then, the elastic energy $E_2(t)$, defined by (43), is a norm of the solution and satisfies (42) with zero boundary term, $BT_2 = 0$. If the coefficient of the artificial dissipation satisfies $\tilde{\varepsilon} := (-1)^{p-1}\varepsilon \geq 0$, the right hand side of (42) is non-positive. Therefore, $E_2(t) \leq E_2(0)$, for $t > 0$, and the problem is well-posed.*

3.1 Discretizing the elastic wave equation with super-grid layers

We discretize (39), (40) on the grid $\xi_i = (i-1)h$, $\eta_j = (j-1)h$, where i and j are integers. The domain sizes and the uniform grid spacing $h > 0$ are defined such that $x_{N_x} = x_{max}$ and $y_{N_y} = y_{max}$. Time is discretized on a grid with constant time step, $\Delta_t > 0$. We denote the displacement at grid point (x_i, y_j) and time level $t_n = n\Delta_t$ by $\mathbf{u}_{i,j}^n = (u_{i,j}^n, v_{i,j}^n)$.

The first two terms on the right hand sides of (39) and (40) are discretized according to

$$L_h^{(u)}\mathbf{u} = \phi^{(x)}G^{(x)}\left(\phi^{(x)}(2\mu+\lambda)\right)u + \phi^{(x)}D^{(x)}(\phi^{(y)}\lambda D^{(y)}v) + \\ \phi^{(y)}D^{(y)}(\phi^{(x)}\mu D^{(x)}v) + \phi^{(y)}G^{(y)}\left(\phi^{(y)}\mu\right)u, \quad (46)$$

and

$$L_h^{(v)}\mathbf{u} = \phi^{(x)}G^{(x)}\left(\phi^{(x)}\mu\right)v + \phi^{(x)}D^{(x)}(\phi^{(y)}\mu D^{(y)}u) + \\ \phi^{(y)}D^{(y)}(\phi^{(x)}\lambda D^{(x)}u) + \phi^{(y)}G^{(y)}\left(\phi^{(y)}(2\mu+\lambda)\right)v, \quad (47)$$

respectively. Here, the grid indices on the grid functions are suppressed to simplify the notation. On vector notation, the discretization is denoted

$$\mathbf{L}_h\mathbf{u}_{i,j}^n = \begin{pmatrix} L_h^{(u)}\mathbf{u}_{i,j}^n \\ L_h^{(v)}\mathbf{u}_{i,j}^n \end{pmatrix}.$$

The finite difference operators $G^{(x)}$ and $D^{(x)}$ in the above formulas act along the first index (ξ-direction). The fourth order accurate operator $G^{(x)}(\mu)w_{i,j}$ approximates $(\mu w_\xi)_\xi(\xi_i, \eta_j)$. Besides operating on a two-dimensional grid function, it is the same as the one-dimensional operator G in (6). The difference operator $D^{(x)}w_{i,j}$ is a fourth order accurate centered approximation of $w_\xi(\xi_i, \eta_j)$. It can be written

$$D^{(x)}w_{i,j} := D_{0x}w_{i,j} - \frac{h^2}{6}D_{0x}D_{+x}D_{-x}w_{i,j} = \\ \frac{1}{12h}\left(-w_{i+2,j} + 8w_{i+1,j} - 8w_{i-1,j} + w_{i-2,j}\right), \quad D_{0x} = \frac{1}{2}(D_{+x} + D_{-x}). \quad (48)$$

Note that the difference operators $G^{(x)}$ and $D^{(x)}$ are *not* boundary modified. As in the one-dimensional case, two ghost points are therefore needed outside $\xi = 0$ and $\xi = x_{max}$.

The fourth order accurate finite difference operators $G^{(y)}(\phi^{(y)}\mu)u$ and $D^{(y)}u$ approximate $(\phi^{(y)}\mu u_\eta)_\eta$ and u_η, respectively. These are one-dimensional operators acting along the second index (η-direction), but with SBP-GP boundary modifications at the $\eta = 0$ boundary, as described in [16]. For this reason, one ghost point is needed outside $\eta = 0$ and two ghost points are needed outside $\eta = y_{max}$.

The artificial dissipation operators in (39) and (40) are discretized in the same way as in the one-dimensional case. The dissipation of order $2p$ is denoted by $Q_{2p}^{(x)}$ in the ξ-direction and $Q_{2p}^{(y)}$ in the η-direction. On vector form, the two-dimensional dissipation becomes

$$\mathbf{Q}_{2p}\mathbf{u} = \begin{pmatrix} \phi^{(x)}Q_{2p}^{(x)}(\sigma^{(x)}\rho)u + \phi^{(y)}Q_{2p}^{(y)}(\sigma^{(y)}\rho)u \\ \phi^{(x)}Q_{2p}^{(x)}(\sigma^{(x)}\rho)v + \phi^{(y)}Q_{2p}^{(y)}(\sigma^{(y)}\rho)v \end{pmatrix}. \quad (49)$$

The dissipation requires p ghost points outside each super-grid boundary. Note that the dissipation in the y-direction does not need any ghostpoints outside $\eta = 0$, because the dissipation coefficient is zero near this boundary, i.e. $\sigma^{(y)} = 0$.

The normal stress boundary conditions (41) are discretized by the fourth order accurate formulas

$$\mu_{i,1} \left(B^{(y)} u_{i,1} + \phi_i^{(x)} D^{(x)} v_{i,1} \right) = \tau_i^{(xy)}, \tag{50}$$

$$(2\mu + \lambda)_{i,1} B^{(y)} v_{i,1} + \lambda_{i,1} \phi_i^{(x)} D^{(x)} u_{i,1} = \tau_i^{(yy)}, \tag{51}$$

for $1 \le i \le N_x$. The boundary operator $B^{(y)} v_{i,1}$ is derived in [16]. It is a 4th order accurate approximation of $v_y(x_i, y_1)$ of the form $\sum_{l=0}^{4} c_l v_{i,l}$, where the stencil coefficient c_0 is nonzero. Therefore, (50) and (51) can be solved for the ghost point values $u_{i,0}$ and $v_{i,0}$.

We define the following boundary operators for two-dimensional grid functions,

$$B_{sg1}(\mathbf{u}) := (\mathbf{u}_{1-\tilde{p},j}, \ldots, \mathbf{u}_{0,j}, \mathbf{u}_{N_x+1,j}, \ldots, \mathbf{u}_{N_x+\tilde{p},j}), \quad 1-\tilde{p} \le j \le N_y + \tilde{p}, \tag{52}$$

$$B_{sg2}(\mathbf{u}) := \left(\mathbf{u}_{i,N_y+1}, \ldots, \mathbf{u}_{i,N_y+\tilde{p}} \right), \qquad 1-\tilde{p} \le i \le N_x + \tilde{p}. \tag{53}$$

As in the one-dimensional case, $\tilde{p} = \max(2, p)$. The boundary conditions (44) and (45) are discretized by

$$B_{sg1}(\mathbf{u}) = 0, \quad B_{sg2}(\mathbf{u}) = 0. \tag{54}$$

Using the above notation, we can write the finite difference approximation of the elastic wave equation with super-grid layers on vector form,

$$\rho \frac{\mathbf{u}^{n+1} - 2\mathbf{u}^n + \mathbf{u}^{n-1}}{\Delta_t^2} = \mathbf{L}_h \mathbf{u}^n + \mathbf{f}^n + \frac{\Delta_t^2}{12} \left(\mathbf{L}_h \ddot{\mathbf{u}}^n + \mathbf{f}_{tt}^n \right) + \varepsilon \mathbf{Q}_{2p} \left(\frac{\mathbf{u}_{i,j}^n - \mathbf{u}_{i,j}^{n-1}}{\Delta_t} \right), \tag{55}$$

where $\mathbf{u}^n = (u^n, v^n)^T$ is subject to the normal stress boundary conditions (50), (51) as well as the Dirichlet conditions $B_{sg1}(\mathbf{u}^n) = 0$ and $B_{sg2}(\mathbf{u}^n) = 0$. In (55), the acceleration is defined by

$$\ddot{\mathbf{u}}_{i,j}^n = \left(\mathbf{L}_h \mathbf{u}_{i,j}^n + \mathbf{f}_{i,j}^n \right) / \rho_{i,j}, \quad 1 \le i \le N_x, \ 1 \le j \le N_y, \tag{56}$$

which is subject to the Dirichlet conditions $B_{sg1}(\ddot{\mathbf{u}}^n) = 0$ and $B_{sg2}(\ddot{\mathbf{u}}^n) = 0$. It is also subject to the normal stress conditions (50), (51), where the boundary forcing functions $(\tau^{(xy)}, \tau^{(yy)})$ are replaced by their second time derivative.

3.2 Energy estimate

In our previous work for second and fourth order accurate methods, e.g., [13, 16], the discrete energy estimate is derived based on the fundamental property

$$(\mathbf{w}, \mathbf{L}_h \mathbf{u})_{hw} = -S_h(\mathbf{w}, \mathbf{u}) + T_h(\mathbf{w}, \mathbf{u}). \tag{57}$$

Here, $(\mathbf{u}, \mathbf{v})_{hw}$ is a weighted scalar product and the bilinear form $S_h(\mathbf{w}, \mathbf{u})$ is symmetric and positive semi-definite. The term $T_h(\mathbf{w}, \mathbf{u})$ is also bilinear and consists of contributions from the boundary. In particular, $T_h(\mathbf{w}, \mathbf{u}) = 0$ when $\mathbf{w}$ satisfies homogeneous Dirichlet conditions, or $\mathbf{u}$ satisfies free surface conditions, see [13, 16] for details.

Our previous estimates hold when the difference operators in $\mathbf{L}_h\mathbf{u}$ are SBP modified at all boundaries of the domain, and when the scalar product is correspondingly weighted near all boundaries. In principle, the same approach could be used to prove a similar estimate for the equations with super-grid far-field closure. However, as we proceed to show, the energy estimate also holds without the boundary modifications of the operators at the super-grid boundaries, if Dirichlet conditions are imposed at several ghost points outside the super-grid boundaries. Avoiding the boundary modified SBP operators at the super-grid boundaries represents a great simplification in implementation and a significant savings in computational cost, especially for three-dimensional problems.

We proceed by proving that the fundamental relation (57) also holds without SBP modifications near the super-grid boundaries. Define the weighted scalar product for real-valued scalar grid functions $u_{i,j}$ and $v_{i,j}$ by

$$(u,v)_{hw} = h^2 \sum_{j=1}^{N_y} \sum_{i=1}^{N_x} \omega_j u_{i,j} v_{i,j}.$$

The corresponding scalar product for real valued vector grid functions $\mathbf{u}_{i,j}$ and $\mathbf{v}_{i,j}$, is

$$(\mathbf{u},\mathbf{v})_{hw} = \left(u^{(x)}, v^{(x)}\right)_{hw} + \left(u^{(y)}, v^{(y)}\right)_{hw}, \quad \mathbf{u} = \begin{pmatrix} u^{(x)} \\ u^{(y)} \end{pmatrix}, \quad \mathbf{v} = \begin{pmatrix} v^{(x)} \\ v^{(y)} \end{pmatrix}.$$

Because the difference operators are SBP modified only at the boundary $\eta = 0$, the weight in the scalar product, ω_j, only depends on j. Furthermore, it is only different from unity for $1 \leq j \leq 4$.

To handle the relation between cross-terms and second derivatives, we need the SBP property of $D^{(x)}u$.

Lemma 5. *Let $u_{i,j}$ and $v_{i,j}$ be real-valued grid functions satisfying the boundary conditions $B_{sg1}(u) = 0$ and $B_{sg1}(v) = 0$. Let $D^{(x)}$ denote the finite difference operator defined by (48). Then,*

$$\left(v, D^{(x)}u\right)_{hw} = -\left(D^{(x)}v, u\right)_{hw}.$$

Proof. See Appendix B.3. □

To prove an energy estimate for the two-dimensional spatial discretization (55) together with boundary conditions (50), (51), and (54), we proceed as follows. We first apply Lemmas 1, 2, and 5, on each operator in x-direction. For the operators in the y-direction, Lemmas 1, 2, and 5 are modified by the summation by parts boundary terms at $\eta = 0$, and become

$$\left(v, G^{(y)}(\mu)u\right)_{hw} = -K_0^{(y)}(v,u) - h\sum_{i=1}^{N_x} \mu_{i,1} v_{i,1} B^{(y)} u_{i,1}, \tag{58}$$

$$\left(v, D^{(y)}u\right)_{hw} = -\left(D^{(y)}v, u\right)_{hw} - h\sum_{i=1}^{N_x} u_{i,1} v_{i,1}, \tag{59}$$

$$\left(v, Q_h^{(y)}u\right)_{hw} = C_0^{(y)}(v,u). \tag{60}$$

Here, the function $K_0^{(y)}(v,u)$ contains a sum of one-dimensional functions $K_0(v,u)$, which is defined in Lemma 1. Similarly, the function $C_0^{(y)}(v,u)$ contains a sum of one-dimensional functions $C_0(v,u)$, which is defined in Lemma 2. The artificial dissipation operator $Q_h^{(y)}$ gives no contributions to the boundary terms at $\eta = 0$, because $\sigma^{(y)}$ is zero there.

Theorem 2. *Let $\mathbf{u}_{i,j}$ and $\mathbf{w}_{i,j}$ be grid functions that satisfy the boundary conditions (50), (51), and* (54)*. The fourth order spatial operators (46), (47) then satisfy*

$$\left(\mathbf{w}, \frac{1}{\phi^{(x)}\phi^{(y)}}\mathbf{L}_h\mathbf{u}\right)_{hw} = -S_h(\mathbf{w},\mathbf{u}), \tag{61}$$

where S_h is bilinear, symmetric, and positive definite. Furthermore, the dissipation operator (49) satisfies

$$\left(\mathbf{w}, \frac{1}{\phi^{(x)}\phi^{(y)}}\mathbf{Q}_{2p}\mathbf{u}\right)_{hw} = C_h(\mathbf{w},\mathbf{u}),$$

where C_h is bilinear, symmetric, and positive semi-definite.

Proof. First, we need the following refinement of (58),

$$\left(v, G^{(y)}(\mu)u\right)_{hw} = -\left(D^{(y)}v, \mu D^{(y)}u\right)_{hw} - \left(v, P^{(y)}(\mu)u\right)_h - h\sum_{i=1}^{N_x}\mu_{i,1}v_{i,1}B^{(y)}u_{i,1}, \tag{62}$$

which was proven in [16]. Here $P^{(y)}(\mu)$ is an operator acting in the y-direction, which is positive definite in the un-weighted scalar product $(u,v)_h$,

$$(u,v)_h = h^2\sum_{i=1}^{N_x}\sum_{j=1}^{N_y}u_{i,j}v_{i,j}.$$

For details, see [16]. The identity corresponding to (62) for the operator in the x-direction does not have a boundary term. The proof is a trivial generalization of the result in Appendix B.1.

To prove (61), we introduce the grid functions $\mathbf{u} = (u^{(x)},\ u^{(y)})^T$, $\mathbf{w} = (w^{(x)},\ w^{(y)})^T$, and write out the components of (61) as

$$\left(\mathbf{w}, \frac{1}{\phi^{(x)}\phi^{(y)}}\mathbf{L}_h\mathbf{u}\right)_{hw} = \left(w^{(x)}, \frac{1}{\phi^{(x)}\phi^{(y)}}L_h^{(u)}\mathbf{u}\right)_{hw} + \left(w^{(y)}, \frac{1}{\phi^{(x)}\phi^{(y)}}L_h^{(v)}\mathbf{u}\right)_{hw}. \tag{63}$$

The first term on the right hand side is expanded as

$$\begin{aligned}\left(w^{(x)}, \frac{1}{\phi^{(x)}\phi^{(y)}}L_h^{(u)}\mathbf{u}\right)_{hw} = \\ \left(w^{(x)}, \frac{1}{\phi^{(y)}}G^{(x)}\left(\phi^{(x)}(2\mu+\lambda)\right)u^{(x)}\right)_{hw} + \left(w^{(x)}, D^{(x)}\lambda D^{(y)}u^{(y)}\right)_{hw} + \\ \left(w^{(x)}, D^{(y)}\mu D^{(x)}u^{(y)}\right)_{hw} + \left(w^{(x)}, \frac{1}{\phi^{(x)}}G^{(y)}\left(\phi^{(y)}\mu\right)u^{(x)}\right)_{hw},\end{aligned} \tag{64}$$

where we have used that $\phi^{(x)}$ does not depend on η_j, and $\phi^{(y)}$ does not depend on ξ_i. Next the summation by parts identites are used on each of the terms in (64). As shown in

Lemmas 1, 2, and 5, there are no boundary terms from operators in the x-direction. The y-direction formulas are given in equations (59), (60), and (62). The resulting expression is

$$\left(w^{(x)}, \frac{1}{\phi^{(x)}\phi^{(y)}} L_h^{(u)}\mathbf{u}\right)_{hw} = -\left(D^{(x)}w^{(x)}, \frac{\phi^{(x)}}{\phi^{(y)}}(2\mu+\lambda)D^{(x)}u^{(x)}\right)_{hw} - \left(w^{(x)}, \frac{1}{\phi^{(y)}}P^{(x)}(\phi^{(x)}(2\mu+\lambda))u^{(x)}\right)_h - \left(D^{(x)}w^{(x)}, \lambda D^{(y)}u^{(y)}\right)_{hw} - \left(D^{(y)}w^{(x)}, \mu D^{(x)}u^{(y)}\right)_{hw} - \left(D^{(y)}w^{(x)}, \frac{\phi^{(y)}}{\phi^{(x)}}\mu D^{(y)}u^{(x)}\right)_{hw} - \left(w^{(x)}, \frac{1}{\phi^{(x)}}P^{(y)}(\phi^{(y)}\mu)u^{(x)}\right)_h - h\sum_{i=1}^{N_x} w_{i,1}^{(x)}\frac{\mu_{i,1}}{\phi_i^{(x)}}\left(\phi_i^{(x)}D^{(x)}u_{i,1}^{(y)} + \phi_1^{(y)}B^{(y)}u_{i,1}^{(x)}\right). \quad (65)$$

By performing a similar expansion of the second term on the right hand side of (63), adding together the results, and completing the squares, we arrive at the final expression

$$\left(\mathbf{w}, \frac{1}{\phi^{(x)}\phi^{(y)}}\mathbf{L}_h\mathbf{u}\right)_{hw} = E_h + P_h + T_h,$$

where

$$E_h = -\left(\phi^{(x)}D^{(x)}w^{(x)} + \phi^{(y)}D^{(y)}w^{(y)}, \frac{\lambda}{\phi^{(x)}\phi^{(y)}}[\phi^{(x)}D^{(x)}u^{(x)} + \phi^{(y)}D^{(y)}u^{(y)}]\right)_{hw} - \left(\phi^{(y)}D^{(y)}w^{(x)} + \phi^{(x)}D^{(x)}w^{(y)}, \frac{\mu}{\phi^{(x)}\phi^{(y)}}[\phi^{(y)}D^{(y)}u^{(x)} + \phi^{(x)}D^{(x)}u^{(y)}]\right)_{hw} - \left(\phi^{(x)}D^{(x)}w^{(x)}, \frac{2\mu}{\phi^{(x)}\phi^{(y)}}[\phi^{(x)}D^{(x)}u^{(x)}]\right)_{hw} - \left(\phi^{(y)}D^{(y)}w^{(y)}, \frac{2\mu}{\phi^{(x)}\phi^{(y)}}[\phi^{(y)}D^{(y)}u^{(y)}]\right)_{hw}, \quad (66)$$

and

$$P_h = -\left(w^{(x)}, \frac{1}{\phi^{(y)}}P^{(x)}(\phi^{(x)}(2\mu+\lambda))u^{(x)}\right)_h - \left(w^{(x)}, \frac{1}{\phi^{(x)}}P^{(y)}(\phi^{(y)}\mu)u^{(x)}\right)_h - \left(w^{(y)}, \frac{1}{\phi^{(y)}}P^{(x)}(\phi^{(x)}\mu)u^{(y)}\right)_h - \left(w^{(y)}, \frac{1}{\phi^{(x)}}P^{(y)}(\phi^{(y)}(2\mu+\lambda))u^{(y)}\right)_h. \quad (67)$$

The boundary terms are

$$T_h = h\sum_{i=1}^{N_x} w_{i,1}^{(y)}\frac{1}{\phi_i^{(x)}}\left(\phi_i^{(x)}\lambda_{i,1}D^{(x)}u_{i,1}^{(x)} + \phi_1^{(y)}(2\mu_{i,1}+\lambda_{i,1})B^{(y)}u_{i,1}^{(y)}\right) + h\sum_{i=1}^{N_x} w_{i,1}^{(x)}\frac{\mu_{i,1}}{\phi_i^{(x)}}\left(\phi_i^{(x)}D^{(x)}u_{i,1}^{(y)} + \phi_1^{(y)}B^{(y)}u_{i,1}^{(x)}\right), \quad (68)$$

which vanishes under the homogeneous boundary condition (50)–(51), because $\phi_1^{(y)} = 1$. Hence, we have

$$S_h(\mathbf{w}, \mathbf{u}) = -E_h - P_h.$$

Here E_h is an approximation of the spatial terms in the elastic energy (43), and P_h is symmetric in its arguments and positive definite when $\mathbf{u} = \mathbf{w}$.

The dissipation operator can similarly be expanded into the four terms

$$\left(\mathbf{w}, \frac{1}{\phi^{(x)}\phi^{(y)}}\mathbf{Q}_{2p}(\mathbf{u})\right)_{hw} = \left(w^{(x)}, \frac{1}{\phi^{(y)}}Q_{2p}^{(x)}(\sigma^{(x)}\rho)u^{(x)}\right)_{hw} + \left(w^{(x)}, \frac{1}{\phi^{(x)}}Q_{2p}^{(y)}(\sigma^{(y)}\rho)u^{(x)}\right)_{hw} + \left(w^{(y)}, \frac{1}{\phi^{(y)}}Q_{2p}^{(x)}(\sigma^{(x)}\rho)u^{(y)}\right)_{hw} + \left(w^{(y)}, \frac{1}{\phi^{(x)}}Q_{2p}^{(y)}(\sigma^{(y)}\rho)u^{(y)}\right)_{hw}. \quad (69)$$

By applying Lemma 2 to each term, we see that the expression is symmetric and positive semi-definite. Note that although Lemma 2 holds in the unweighted norm, and (69) uses the weighted norm, there is no difficulty because the y-direction operators in (69) are zero near the boundary $\eta = 0$, where the norm is weighted. □

The discretization of the elastic wave equation with super-grid layers, (55), can be written in matrix form as (18), with symmetric positive (semi-)definite matrices K and C_{2p}. Similar to the one-dimensional case, these matrices are defined through $S_h(\mathbf{w}, \mathbf{u}) = \mathbf{w}^T K \mathbf{u}$ and $C_h(\mathbf{w}, \mathbf{u}) = \mathbf{w}^T C_{2p} \mathbf{u}$. Furthermore, in the two-dimensional case, the matrix Φ is still diagonal, with elements $\phi^{(x)}\phi^{(y)}$. For example,

$$\mathbf{L}_h\mathbf{u} = \phi^{(x)}\phi^{(y)}\left(\frac{1}{\phi^{(x)}\phi^{(y)}}\mathbf{L}_h\mathbf{u}\right) = -\phi^{(x)}\phi^{(y)}K\mathbf{u} = -\Phi K\mathbf{u}.$$

The remaining terms in (55) can be rewritten similarly, allowing the finite difference scheme for the elastic wave equation to be cast in the same matrix formulation as the scalar wave equation, i.e. (18). Theorem 1 therefore applies also to (55), and we obtain our main result.

Theorem 3. *The finite difference scheme (55) with zero forcing* $\mathbf{f}^n = 0$ *and homogeneous boundary conditions (50), (51), and* (54)*, has a non-increasing discrete energy*

$$e^{n+1/2} \leq e^{n-1/2} \leq \ldots \leq e^{1/2}.$$

The discrete energy, corresponding to (20)*, is a norm of the solution when the time step satisfies the inequalities corresponding to (21) and (22). Therefore, the scheme (55) is stable.*

4 Numerical experiments

4.1 Lamb's problem

Lamb [8] derived an analytic solution of the elastic wave equation in a homogeneous half-space, subject to an impulsive vertical point forcing applied on the free surface boundary. Many generalizations have been made to Lamb's original derivation, see for example [11] or [6]. Here we focus on the case with $\lambda = \mu$ (Poisson ratio 1/4) where the evaluation of the analytic solution is somewhat simplified.

We shall solve Lamb's problem numerically and take the domain of interest to be $\ell \le x \le 4+\ell$, $\ell \le y \le 4+\ell$, $0 \le z \le 2$. The forcing is given by the singular point force

$$\mathbf{f}(\mathbf{x},t) = \begin{pmatrix} 0 \\ 0 \\ g(t)\delta(\mathbf{x}-\mathbf{x}_0) \end{pmatrix},$$

where $\delta(\mathbf{x}-\mathbf{x}_0)$ is the Dirac distribution centered at $\mathbf{x}_0 = (2+\ell, 2+\ell, 0)$. The point force is discretized in space by using the technique described in [14]. The time function satisfies

$$g(t) = \begin{cases} 16384\, t^7(1-t)^7, & 0 < t < 1, \\ 0, & \text{otherwise.} \end{cases} \tag{70}$$

The source time function $g(t)$ is six times continuously differentiable, symmetric around $t = 0.5$, where $g(0.5) = 1$. The smoothness in time of the point forcing translates to smoothness in space of the solution after the point force has stopped acting, i.e., for times $t > 1$ in this case. Super-grid layers of width ℓ are added to all sides of the domain of interest, except along $z = 0$, where homogeneous free surface conditions corresponding to (50) and (51) are imposed. We choose the units such that the homogeneous elastic material has the properties $\mu = \lambda = \rho = 1$. The computational domain is taken to be $0 \le x \le 4+2\ell$, $0 \le y \le 4+2\ell$, $0 \le z \le 2+\ell$.

Figure 3 shows the numerical solution at three different times when the super-grid layer has thickness $\ell = 2$ and the grid size is $h = 0.02$. Here the magnitude of the displacement, $\sqrt{u^2+v^2+w^2}$, is plotted. The top left and right subfigures show a strong Rayleigh surface wave as well as a weak outward propagating compressional wave moving with speed $c_p = \sqrt{3}$. A shear wave of intermediate strength moves outwards with speed $c_s = 1$. For a material with $\mu = \lambda = 1$ it can be shown that the Rayleigh surface wave propagates with phase velocity $c_r \approx 0.92$. Because the wave speed in each direction of the super-grid layers is proportional to the value of the corresponding stretching function, the solution slows down and becomes compressed inside the super-grid layers. Also note that the wave fronts tend towards a square shape as time progresseses. We remark that no artificially reflected waves are visible within the domain of interest, here outlined with a dashed line.

Mooney [11] gives explicit expressions for the analytical solution of Lamb's problem on the surface $z = 0$ in terms of a Green's function, $G(t)$. The z-component of the solution at a point on the surface satisfies

$$w(x,y,0,t) = \frac{K}{r}\int_0^t g'(t-\tau)\, G\left(\frac{\tau}{r}\right)\, d\tau, \tag{71}$$

where $r = \sqrt{x^2+y^2}$, and

$$G(\xi) = \begin{cases} 0, & \xi < 1/\sqrt{3}, \\ c_1 + c_2/\sqrt{\gamma^2-\xi^2} + c_3/\sqrt{\xi^2-b^2} + c_4/\sqrt{\xi^2-1/4}, & 1/\sqrt{3} < \xi < 1, \\ c_5 + c_6/\sqrt{\gamma^2-\xi^2}, & 1 < \xi < \gamma, \\ c_7, & \gamma < \xi. \end{cases} \tag{72}$$

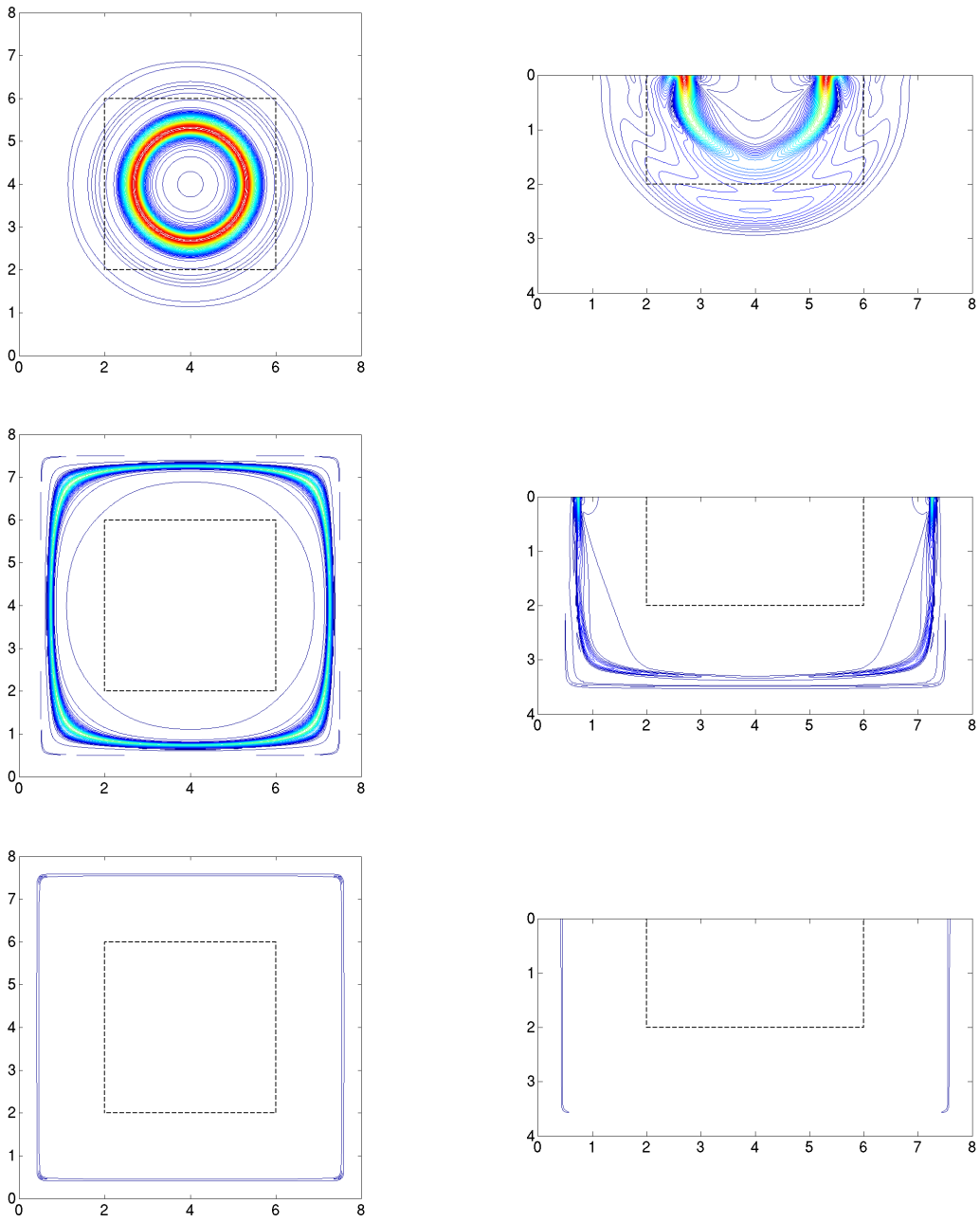

Figure 3: Magnitude of the displacement for Lamb's problem at times 2, 5, and 12 (top to bottom) in the $z = 0$ plane (left) and the $y = 4$ plane (right). The contour levels are the same in all plots and are spaced between 0.005 (dark blue) and 0.505 (red) with step size 0.01.

The values of the constants K, c_i, b, and γ are given in [11], with $b \approx 0.563$ and $\gamma \approx 1.0877$. Hence all integrands are non-singular, except in the third case of (72), which has an integrable singularity at $\xi = \gamma$. When g is given by (70), we obtain the exact solution as a sum of terms that either are integrals of polynomials, or have the form

$$\int \frac{P(\xi)}{\sqrt{\xi^2 - a^2}}\, d\xi. \tag{73}$$

where $P(\xi)$ is a polynomial in ξ. Analytical expressions for integrals of the form (73) can be found, but their numerical evaluation is very sensitive to round-off errors, due to the high polynomial order of P. These analytical formulas are therefore inadequate for numerically calculating the exact solution. Instead, we numerically evaluate the convolution integral (71) using the Quadpack library from the Netlib website [12]. This approach turns out to be much better conditioned, and permits us to evaluate the formula (71) to within approximately 12 decimal places.

In Figures 4–6 we show the max norm of the error in the w-component of the solution, as function of time. The norm is evaluated where the analytical solution is available, i.e., on the surface $z = 0$, for $\ell \leq x \leq 4 + \ell$, $\ell \leq y \leq 4 + \ell$. Note that the point force makes the exact solution unbounded at $\mathbf{x} = \mathbf{x}_0$ for $0 < t < 1$, making the max norm of the error undefined. A few grid points near $\mathbf{x}_0$ are therefore excluded from the norm calculation. Three different computations, corresponding to grid sizes $h = 0.04$ (blue), $h = 0.02$ (red), and $h = 0.01$ (black) are shown. In all computations, three different regimes of the error can be distinguished. First, for $0 < t < 1$ the point force is active, and the numerical solution has a large error near $\mathbf{x}_0$, where the exact solution is unbounded. No reduction of the max norm of the error is obtained as the grid is refined. Secondly, for times $1 < t < 4$ the forcing is zero, and the solution error is dominated by truncation errors from the fourth order accurate difference scheme. Here, fourth order convergence is obtained as the grid is refined. The slowest wave in the solution is the surface wave, propagating at phase velocity $c_r \approx 0.92$. The surface waves therefore leaves the domain around $t \approx 1 + 2\sqrt{2}/0.92 \approx 4.08$. After that time, the exact solution is zero, and the error is dominated by effects from the super-grid far-field closure. Hence, the behavior of the error for $t > 4$ depends on the properties of super-grid layer. The simulations are run to time 12.

Figure 4 shows the influence of the width of the super-grid layer, ℓ. The left subfigure is computed with $\ell = 1$ and the right subfigure with $\ell = 2$. In both cases, a sixth order dissipation is used in the super-grid layer. The right subfigure of Figure 5 shows the same computation, but with $\ell = 4$. As expected, the error for $t \leq 4$ is independent of ℓ. For $t > 4$, the error for each grid size becomes smaller when ℓ is made larger. For each fixed ℓ, the error also decreases at a faster rate as the grid is refined when ℓ is larger.

Figure 5 compares fourth order dissipation with sixth order dissipation in the super-grid layer. On the coarser grids, the two dissipations give comparable errors, but as the grid is refined, the sixth order dissipation shows superior performance. The formal order of accuracy in the layer is three for the fourth order dissipation, and five for the sixth order dissipation. Because information propagates from the layer into the domain of interest, we expect the overall convergence rate to be reduced to third order with the fourth order dissipation. However, Figure 5 indicates that this third order error is very small, and only becomes significant on a very fine grid.

Finally, Figure 6 shows the result of using a fixed number of grid points in the super-grid layer. This means that the layer width ℓ becomes smaller as the grid is refined.

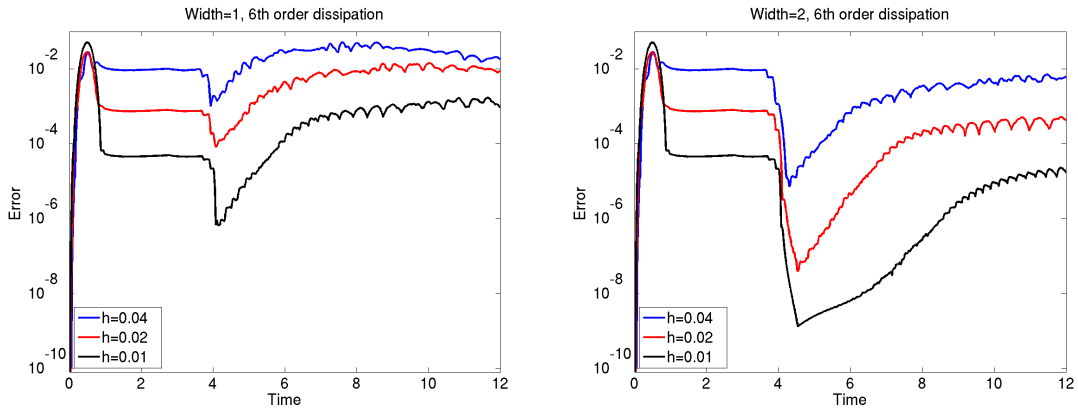

Figure 4: *Max error in the vertical component of Lamb's problem with sixth order artificial dissipation, where the width of the super-grid layer is* $\ell = 1$ *(left) and* $\ell = 2$ *(right).*

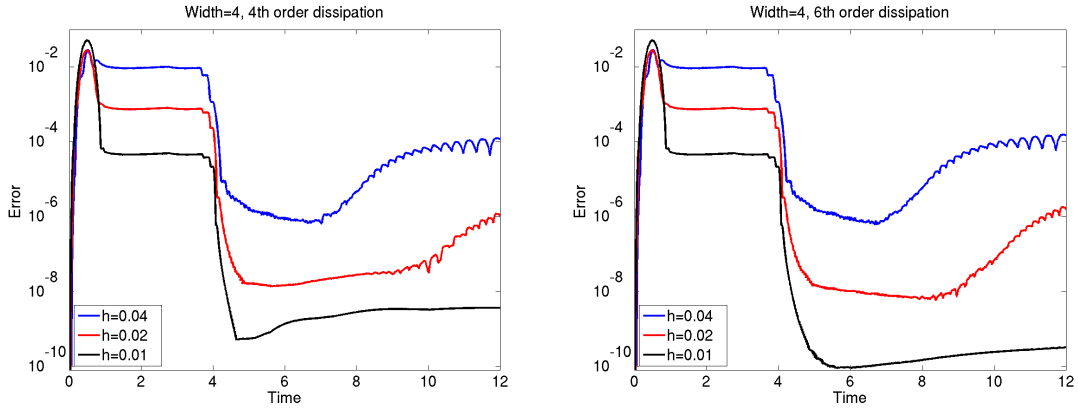

Figure 5: *Max error in the vertical component of Lamb's problem, where the width of the super-grid layer is* $\ell = 4$*. Fourth order artificial dissipation (left) compared with sixth order artificial dissipation (right).*

In this computation, 50 grid points are used in the layer. Hence, $h = 0.04$ (blue) gives $\ell = 2$, $h = 0.02$ (red) has $\ell = 1$, and $h = 0.01$ (black) corresponds to $\ell = 0.5$. Clearly, this strategy does not perform well. Note that the errors for all grid sizes tend to approximately the same value as time increases.

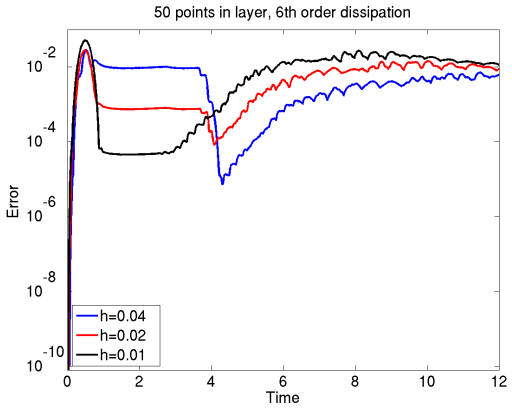

Figure 6: *Max error in the vertical component of Lamb's problem with sixth order artificial dissipation, when the width of the super-grid layer equals 50 grid sizes, i.e. the physical thickness of the super-grid layer becomes thinner as the grid is refined.*

4.2 The layer over half-space problem

The layer over half-space (LOH1) problem, defined in [5], is a popular test case for seismic wave equation solvers. The material in this model consists of a top layer, extending from depth $z = 0$ to $z = 1000$, where the material velocities and the density are $c_p = 4000$, $c_s = 2000$, and $\rho = 2600$, respectively. In the half space $z > 1000$, the material properties are $c_p = 6000$, $c_s = 3464$, and $\rho = 2700$. The domain of interest in the LOH1 problem is $0 \le x \le 30000$, $0 \le y \le 30000$, and $0 \le z \le 17000$. A free surface boundary condition is imposed along the top boundary, $z = 0$. Super-grid layers of width ℓ are added on all other sides of the domain of interest. This results in the computational domain $-\ell \le x \le 30000 + \ell$, $-\ell \le y \le 30000 + \ell$, and $0 \le z \le 17000 + \ell$. The forcing in the LOH1 problem is the point moment tensor source,

$$\mathbf{f}(\mathbf{x}, t) = g(t) \begin{pmatrix} 0 & m_{xy} & 0 \\ m_{xy} & 0 & 0 \\ 0 & 0 & 0 \end{pmatrix} \nabla\delta(\mathbf{x} - \mathbf{x}_0),$$

located at $(x_0,\ y_0,\ z_0) = (15000,\ 15000,\ 2000)$, with amplitude $m_{xy} = 10^{18}$. The source time function is the Gaussian

$$g(t) = \frac{1}{2\pi\sigma} e^{(t-t_0)^2/2\sigma^2}, \quad \sigma = 0.06, \quad t_0 = 0.36.$$

The elastic wave equation is integrated from homogeneous initial data at $t = 0$ to time $t = 9$. All computations are made with the super-grid layer thickness $\ell = 2500$. The

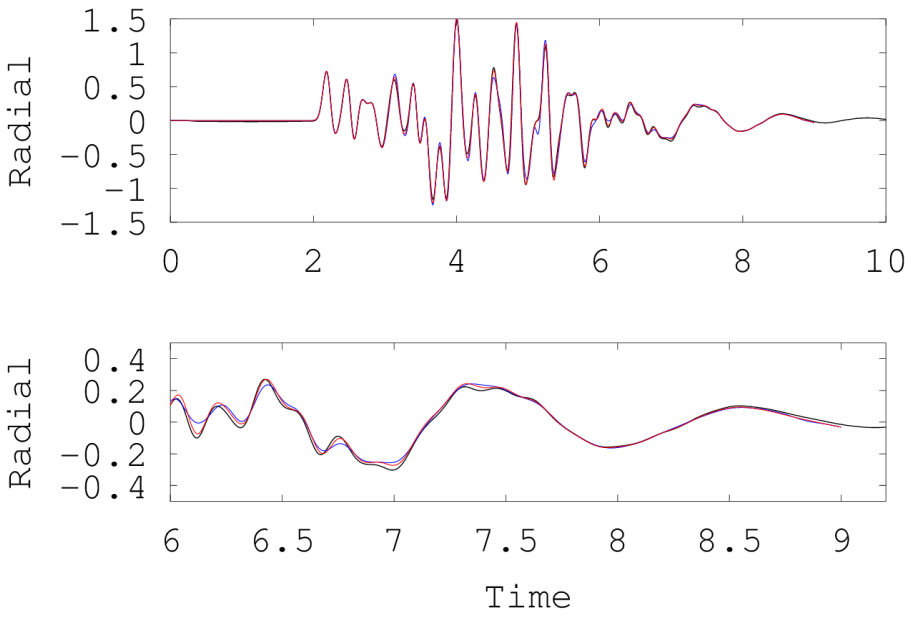

Figure 7: *Radial solution component vs. time for the LOH1 test problem. The solution is recorded at* (21000, 23000, 0)*. The numerical solutions with grid sizes* $h = 50$ *(blue),* $h = 25$ *(red), are compared to a semi-analytical solution (black). The lower subfigure shows a close up for times* $6 \leq t \leq 9$*.*

solution is recorded as function of time at the location $\mathbf{x}_r = (21000, 23000, 0)^T$. Note that by time 9, the fastest compressional wave has traveled the distance $6000(9-0.36) = 51,840$, which is well beyond the distance from the source to the boundary of the computational domian, and back into the domain of interest. Evaluating the error up to time 9 should therefore be a good test of the reflection properties of the super-grid layer for the LOH1 problem.

Figure 7 displays a comparison between the semi-analytical solution and two numerical solutions with grid sizes $h = 50$ and $h = 25$, respectively. To save space, we only show the radial component of the solution vector $\mathbf{u}$, i.e., $u_r = 0.6u + 0.8v$. The accuracy in the tangential and vertical components is similar, or better. We conclude that the agreement between the computed and 'exact' semi-analytical solutions is good throughout the simulation, with no visible deterioration in accuracy due to the super-grid far-field closure.

5 Conclusions

We have developed a super-grid modeling technique for solving the elastic wave equation in two-dimensional half-plane and three-dimensional half-space domains. The super-grid technique is based on a coordinate stretching combined with the explict addition of a dissipation operator. The change of coordinates transforms a very large physical domain to a significantly smaller computational domain, where the wave equation is solved numerically

on a regular grid. A high order artificial dissipation operator is added in layers near the boundaries of the computational domain. It damps out waves that become poorly resolved because of the coordinate stretching.

Stability of the super-grid method follows for any approximation that is stable when discretized on a curvilinear grid, if also the dissipation term is discretized in a stable way, e.g., by using semi-bounded difference operators. In particular, we have proven that the super-grid technique leads to a stable numerical method with decreasing energy, when used together with our fourth order summation-by-parts scheme [16]. The stability is valid for heterogeneous material properties and a free surface boundary condition on one side of the domain. We have proven that the summation by parts property holds when a centered finite difference stencil is combined with homogeneous Dirichlet conditions at several ghost points outside of the far-field boundaries. Therefore, the coefficients in the finite difference stencils need only be boundary modified near the free surface. This allows for improved computational efficiency and significant simplifications of the implementation in multi-dimensional domains.

One very desirable property of the super-grid method is that, with a wide enough layer, the modeling error from truncating the domain can be made as small as the wave propagation errors due to the truncation errors of the interior scheme. This allows the total error in the solution to converge with full order of accuracy as the grid size tends to zero. As shown in the numerical experiments, this is possible with a damping layer that is considerably thinner than the trivial layer, which would be as wide as the distance traveled by the fastest wave over the duration of the entire simulation. However, while the modeling error is reduced by making the super-grid layer thicker, it also increases the computational cost and storage requirements of the simulation. There is therefore a trade-off between computational cost and accuracy of the solution, which is tunable by only changing one parameter: the width of the super-grid layers.

The super-grid technique should be straightforward to generalize to higher order of accuracy. The $2p$ order dissipation operator gives a $2p-1$ order truncation error in the super-grid layers. Since these errors can propagate into the domain of interest, it is necessary to choose p such that $2p-1$ is larger than or equal to the expected convergence rate of the difference scheme. Additional extensions of the current work could include a more detailed analysis of the modeling error from truncating the domain, and a mathematical proof of our numerical observation that the solution converges with optimal rate, as the grid size tends to zero, if the super-grid layer is sufficiently wide.

A Construction of the stretching function

We base to construction of the stretching function on a function $\phi_0(\xi)$, which transitions smoothly from the value ϵ_L to one over the interval $[0,1]$, i.e.,

$$\phi_0(\xi) = \begin{cases} \epsilon_L, & \xi \le 0, \\ \epsilon_L + (1-\epsilon_L)P(\xi), & 0 < \xi < 1, \\ 1, & \xi \ge 1. \end{cases} \tag{74}$$

The function $P(\xi)$ should be a smooth monotonically increasing function of ξ. Here we use the polynomial function $P(\xi) = \xi^5(126 - 420\xi + 540\xi^2 - 315\xi^3 + 70\xi^4)$, which makes $\phi_0(\xi)$ four times continously differentiable.

The width of each super-grid layer is $\ell > 0$. Let the domain of interest be $x_1 \le x \le x_2$. A stretching function with super-grid layers both at $x < x_1$ and $x > x_2$ is given by

$$\phi(x) = \begin{cases} \phi_0((x - (x_1 - \ell))/\ell), & x_1 - \ell \le x < x_1, \\ 1, & x_1 \le x \le x_2, \\ \phi_0((x_2 + \ell - x)/\ell), & x_{max} - \ell < x \le x_{max}. \end{cases} \tag{75}$$

B Summation by parts relations

B.1 Properties of $G(\mu)u$

We simplify the notation by first analyzing the function $K_1(v,u) := (v, G(\mu)u)_{h1}$. The finite difference operator (6) can be written as a sum of three difference operators

$$G(\mu)u_j = D^{(x1)}\left(\mu_j D^{(x1)} u_j\right) + \frac{h^4}{18} D_+ D_- D_+ \left(\tilde{\mu}_j D_- D_+ D_- u_j\right) - \frac{h^6}{144}\left(D_+ D_-\right)^2 \left(\mu_j \left(D_+ D_-\right)^2 u_j\right), \tag{76}$$

where $\tilde{\mu}_j = (\mu_j + \mu_{j-1})/2$. Here, D_+ and D_- denote the standard forward and backward divided difference operators. Furthermore, the term $D^{(x1)} w_j$ is a centered fourth order accurate approximation of $w_\xi(\xi_j)$. It can be written

$$D^{(x1)} w_j := D_0 w_j - \frac{h^2}{6} D_0 D_+ D_- w_j, \quad D_0 = \frac{1}{2}(D_+ + D_-). \tag{77}$$

In the following we set $N = N_x$.

We want to analyze $G(\mu)u_j$ for $j = 1, 2, \ldots, N$. Since $G(\mu)u_j$ is a five point formula, its values at the interior points $1 \le j \le N$ are only influenced by u_q for $-1 \le q \le N+2$. The boundary condition $B_{sg}(u) = 0$ sets $u_{-1} = u_0 = 0$ and $u_{N+1} = u_{N+2} = 0$. However, we can impose boundary conditions at additional ghost points without changing $G(\mu)u_j$ for $j = 1, 2, \ldots, N$. In particular, we choose to replace $B_{sg}(u) = 0$ and $B_{sg}(v)$ by imposing homogeneous Dirichlet conditions at four ghost points

$$u_{-3} = u_{-2} = u_{-1} = u_0 = 0, \quad v_{-3} = v_{-2} = v_{-1} = v_0 = 0, \tag{78}$$

$$u_{N+1} = u_{N+2} = u_{N+3} = u_{N+4} = 0, \quad v_{N+1} = v_{N+2} = v_{N+3} = v_{N+4} = 0. \tag{79}$$

It is convenient to analyze $G(\mu)u_j$ by studying each term on the right hand side of (76) independently. We focus on the properties of $G(\mu)u_j$ near the left boundary, and we extend the grid functions to the semi-infinite domain $j \ge -3$ subject to the boundary conditions (78). We modify the scalar product to be

$$(u, v)_{h0} = h \sum_{j=1}^{\infty} u_j v_j. \tag{80}$$

In this scalar product, the basic forward, backward and centered divided difference operators satisfy the SBP parts identities

$$\begin{aligned} (v, D_+ w)_{h0} &= -(D_- v, w)_{h0} - w_1 v_0, \\ (v, D_- w)_{h0} &= -(D_+ v, w)_{h0} - w_0 v_1, \\ (v, D_0 w)_{h0} &= -(D_0 v, w)_{h0} - \frac{1}{2}(w_0 v_1 + w_1 v_0). \end{aligned} \tag{81}$$

Repeated use of these identities and boundary condition (78) lead to the relations

$$\left(v, D^{(x1)}(\mu D^{(x1)}u)\right)_{h0} = -\left(D^{(x1)}v, \mu D^{(x1)}u\right)_{h0} - J_1, \tag{82}$$

$$(v, D_+D_-D_+\left(\tilde{\mu}D_-D_+D_-u\right))_{h0} = -\left(D_-D_+D_-v, \tilde{\mu}D_-D_+D_-u\right)_{h0} - J_2, \tag{83}$$

$$\left(v, (D_+D_-)^2\left(\mu\left(D_+D_-\right)^2 u\right)\right)_{h0} = \left((D_+D_-)^2 v, \mu\left(D_+D_-\right)^2 u\right)_{h0} + J_3. \tag{84}$$

The boundary terms satisfy

$$\begin{aligned}
J_1 &= \frac{1}{144h}\left(\mu_0(u_2 - 8u_1)(v_2 - 8v_1) + \mu_{-1}u_1v_1\right), \\
J_2 &= \frac{1}{h^5}\left(\mu_{-1/2}u_1v_1\right), \\
J_3 &= \frac{1}{h^7}\left(\mu_{-1}u_1v_1 + \mu_0(u_2 - 4u_1)(v_2 - 4v_1)\right).
\end{aligned}$$

By collecting terms,

$$\begin{aligned}
(v, G(\mu)u)_{h0} = -\left(D^{(x1)}v, \mu D^{(x1)}u\right)_{h0} - \frac{h^4}{18}\left(D_-D_+D_-v, \tilde{\mu}D_-D_+D_-u\right)_{h0} - \\
\frac{h^6}{144}\left((D_+D_-)^2 v, \mu\left(D_+D_-\right)^2 u\right)_{h0} - J,
\end{aligned} \tag{85}$$

where the boundary term satisfies $J = J_1 + h^4J_2/18 + h^6J_3/144$. All terms in (85) are symmetric in u and v. Since $\mu > 0$, all terms are negative or zero if $u = v$. The contributions from the right boundary can be analyzed in the same way. Collecting all contributions to $(v, G(\mu)u)_{h1}$ shows that the function K_1 is symmetric, i.e.,

$$K_1(v, u) := -\left(v, G(\mu)u\right)_{h1}, \quad K_1(v, u) = K_1(u, v).$$

From the above construction, it is clear that $K_1(u, u) \geq 0$. It remains to show that $K_1(u, u)$ is positive definite, i.e., $K_1(u, u) = 0$ if and only if $u = 0$. Obviously, $K_1(u, u) = 0$ if $u = 0$. Because $K_1(u, u)$ is a sum of non-negative terms, it can only be zero if each term is zero. We choose to study the term

$$T_1(u) := \left(D_-D_+D_-u, \tilde{\mu}D_-D_+D_-u\right)_{h1} = h\sum_{j=1}^{N}\mu_{j-1/2}\left(D_-D_+D_-u_j\right)^2.$$

The difference equation $D_-D_+D_-u_j = 0$ has the general solution $u_j = \alpha + j\beta + j^2\gamma$ where α, β, and γ are constants. Because $T_1(u)$ only depends on the ghost point values u_{-1}, u_0, and u_{N+1}, the boundary condition $B_{sg}(u) = 0$ gives the linear system

$$\alpha - \beta + \gamma = 0, \tag{86}$$

$$\alpha = 0, \tag{87}$$

$$\alpha + (N+1)\beta + (N+1)^2\gamma = 0. \tag{88}$$

It is straight forward to see that this system only has the trivial solution $\alpha = \beta = \gamma = 0$. We conclude that $T_1(u) = 0$ if and only if $u = 0$. Hence, $K_1(u, u) = 0$ if and only if $u = 0$.

Since $\phi_j = \phi(\xi_j) \geq \varepsilon_L > 0$, the same arguments apply to the function $K_0(v, u) = (v, G(\phi\mu)u)_{h1}$. This proves the lemma.

B.2 The artificial dissipation operator Q_{2p}

We apply the same technique as in section B.1 and start by studying the boundary terms due to the left boundary, using the scalar product (80). For a fourth order dissipation, $p = 2$, and we define $w_j = \sigma_j \rho_j D_+ D_- u_j$. We have,

$$(v, Q_4 u)_{h0} = (v, D_+ D_- w)_{h0}.$$

Combining the first two summation by parts rules in (81) gives

$$(v, D_+ D_- w)_{h0} = (D_+ D_- v, w)_{h0} - v_0 D_- w_1 + w_0 D_- v_1.$$

Because v satisfies the boundary condition $B_{sg}(v) = 0$, we have $v_0 = 0$. Therefore, the first boundary term is zero. For the second boundary term we have $D_- v_1 = v_1/h$. It can be further simplified because $B_{sg}(u) = 0$, so $u_{-1} = u_0 = 0$. Therefore, $w_0 = \sigma_0 \rho_0 u_1 / h^2$ and we obtain

$$(v, Q_4 u))_{h0} = (v, D_+ D_- w)_{h0} = (D_+ D_- v, \sigma \rho D_+ D_- u)_{h0} + v_1 u_1 \frac{\sigma_0 \rho_0}{h^3}.$$

All terms on the right hand side are symmetric in u and v. Furthermore, they are non-negative when $u = v$. Hence, there is a function $C_0(u, v)$ that does not depend on the ghost point values of u or v, such that

$$(v, Q_4 u))_{h0} = C_0(v, u), \quad C_0(u, v) = C_0(v, u), \quad C_0(u, u) \geq 0.$$

The influence of the right boundary can be analyzed in the same way. The same approach applies to all dissipation operators of order $2p$, $p \geq 1$. This proves the lemma.

B.3 Anti-symmetry of $D^{(x)}$

We first prove the corresponding lemma for the 1-D operator (77), where u and v are 1-D grid functions satisfying the boundary conditions $B_{sg}(u) = 0$ and $B_{sg}(v) = 0$. By expanding the terms in the scalar product and rearranging them,

$$\begin{aligned}
\left(v, D^{(x1)} u\right)_{h1} &= \frac{1}{12} \sum_{i=1}^{N} v_i (u_{i-2} - 8u_{i-1} + 8u_{i+1} - u_{i+2}) \\
&= \frac{1}{12} \left[u_{-1} v_1 + u_1 v_{-1} + u_0(-8v_1 + v_2) + v_0(-8u_1 + u_2)\right] + \\
&\qquad \frac{1}{12} \sum_{i=1}^{N} u_i (-v_{i-2} + 8v_{i-1} - 8v_{i+1} + v_{i+2}) + \\
&\frac{1}{12} \left[-u_{N+2} v_N - v_{N+2} u_N + u_{N+1}(8v_N - v_{N-1}) + v_{N+1}(8u_N - u_{N-1})\right]. \quad (89)
\end{aligned}$$

The boundary terms are equal to zero because $B_{sg}(u) = 0$ and $B_{sg}(v) = 0$ imply $u_{-1} = u_0 = v_{-1} = v_0 = 0$ and $u_{N+2} = u_{N+1} = v_{N+2} = v_{N+1} = 0$. Hence, we obtain

$$\left(v, D^{(x1)} u\right)_{h1} = - \left(D^{(x1)} v, u\right)_{h1}.$$

Trivial generalizations extend the proof to two-dimensional grid functions.

References

[1] D. Appelö and T. Colonius. A high order super-grid-scale absorbing layer and its application to linear hyperbolic systems. *J. Comput. Phys.*, 228:4200–4217, 2009.

[2] E. Bécache, S. Fauqueux, and P. Joly. Stability of perfectly matched layers, group velocities and anisotropic waves. *J. Compt. Phys.*, 188:399–433, 2003.

[3] J. P. Berenger. A perfectly matched layer for the absorption of electromagnetic waves. *J. Comput. Phys.*, 114:185–200, 1994.

[4] R. Clayton and B. Engquist. Absorbing boundary conditions for acoustic and elastic wave equations. *Bull. Seismo. Soc. Amer.*, 67, 1977.

[5] S. M. Day, J. Bielak, D. Dreger, S. Larsen, R. Graves, A. Pitarka, and K. B. Olsen. Test of 3D elastodynamic codes: Lifelines project task 1A01. Technical report, Pacific Earthquake Engineering Center, 2001.

[6] A. Cemal Eringen and Erdoğan S. Şuhubi. *Elastodynamics, Volume II.* Elsevier, 1975.

[7] R. L. Higdon. Radiation boundary conditions for elastic wave propagation. *SIAM J. Numer. Anal.*, 27:831–870, 1990.

[8] Horace Lamb. On the propagation of tremors over the surface of an elastic solid. *Phil. Trans. Roy. Soc. London, Ser. A*, 203, 1904.

[9] K. Mattsson, F. Ham, and G. Iaccarino. Stable and accurate wave-propagation in discontinuous media. *J. Comput. Phys.*, 227:8753–8767, 2008.

[10] K. Mattsson and J. Norström. Summation by parts operators for finite difference approximations of second derivatives. *J. Comput. Phys.*, 199:503–540, 2004.

[11] Harold M. Mooney. Some numerical solutions for Lamb's problem. *Bull. Seismo. Soc. Amer.*, 64, 1974.

[12] Netlib. Repository of scientific computing software. `http://www.netlib.org`.

[13] N. A. Petersson and B. Sjögreen. An energy absorbing far-field boundary condition for the elastic wave equation. *Comm. Comput. Phys.*, 6:483–508, 2009.

[14] N. A. Petersson and B. Sjögreen. Stable grid refinement and singular source discretization for seismic wave simulations. *Comm. Comput. Phys.*, 8(5):1074–1110, November 2010.

[15] B. Sjögreen and N. A. Petersson. Perfectly matched layers for Maxwell's equations in second order formulation. *J. Comput. Phys.*, 209:19–46, 2005.

[16] B. Sjögreen and N. A. Petersson. A fourth order accurate finite difference scheme for the elastic wave equation in second order formulation. *J. Sci. Comput.*, 52:17–48, 2012. DOI 10.1007/s10915-011-9531-1.

[17] E. A. Skelton, S. D. M. Adams, and R. V. Craster. Guided elastic waves and perfectly matched layers. *Wave Motion*, 44:573–592, 2007.